Land conservation and large-scale renewable energy systems are simultaneously possible in Brazil

Conde Santos Borba, Paula; Cabral de Sousa, Wilson; Pfenninger, Stefan

DOI
10.1016/j.oneear.2025.101520

Publication date
2025

Document Version
Final published version

Published in
One Earth

One Earth

Article

Land conservation and large-scale renewable energy systems are simultaneously possible in Brazil

Graphical abstract

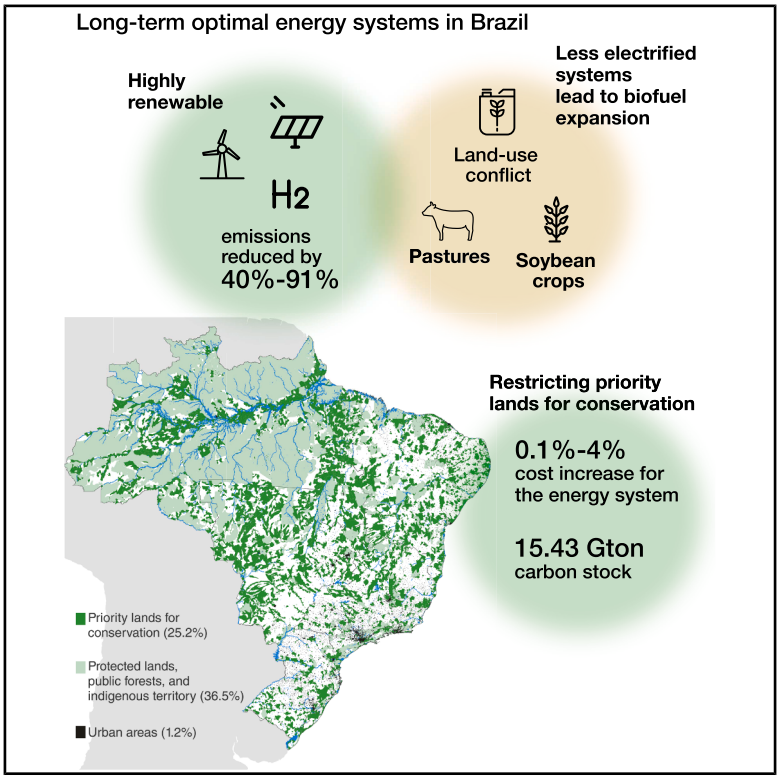

Highlights

- Brazil can deploy large-scale renewables without harming conservation-priority lands
- Restricting the use of conservation-priority lands raises energy costs by 4%
- CO_2 emissions can be cut by up to 91% and 770 Mt CO_2/year sequestered via reforestation
- Biofuel-led renewable expansion will largely overlap degraded pastures

Authors

Paula Conde Santos Borba, Wilson Cabral de Sousa, Jr., Stefan Pfenninger

Correspondence

paula.borba@inpe.br

In brief

Brazil's rich but sensitive ecosystems face uncertainty amid deep decarbonization efforts that could drive significant land-use changes. Here, using a spatially explicit energy system model, we demonstrate that, with strategic, location-wise planning of renewable energy, including solar, wind, and biofuels, Brazil can supply extensive renewable electricity while safeguarding key conservation areas without major cost increases. Protecting and restoring these lands increases carbon sinks, delivering integrated co-benefits for energy, climate, and ecology.

Conde Santos Borba et al., 2025, One Earth *8*, 101520
November 21, 2025
https://doi.org/10.1016/j.oneear.2025.101520

CellPress

One Earth

CellPress

Article

Land conservation and large-scale renewable energy systems are simultaneously possible in Brazil

Paula Conde Santos Borba,[1,2,3,4,5,*] Wilson Cabral de Sousa, Jr.,[1] and Stefan Pfenninger[3]
[1]Department of Civil Engineering, Aeronautics Institute of Technology (ITA), São Paulo, Brazil
[2]Laboratory of Modeling and Studies on Renewable Energy Resources, National Institute for Space Research (INPE), São Paulo, Brazil
[3]Faculty of Technology, Policy and Management, Delft University of Technology, Delft, the Netherlands
[4]Federal University of São Paulo, Sea Science Department, Santos, São Paulo, Brazil
[5]Lead contact
*Correspondence: paula.borba@inpe.br
https://doi.org/10.1016/j.oneear.2025.101520

SCIENCE FOR SOCIETY Brazil has a well-established history of renewable energy development, particularly in the production of biofuels. The biofuel pathway, however, raised significant concerns, mainly due to land-use conflicts that have caused socioecological challenges, considering the country's stewardship of many globally rich ecosystems. As Brazil moves toward net-zero emissions, expanding biofuels alongside solar and wind power will intensify land-use competition. A critical yet unresolved science-policy question is how to balance large-scale renewable energy deployment without compromising ecological integrity. Using a high-resolution, spatially explicit energy system model, we demonstrate the feasibility of a cost-effective, extensive renewable energy network that protects priority conservation areas while enabling an additional 770 million tons of annual CO_2 sequestration. Our study provides actionable strategies for policymakers and stakeholders to reconcile the expansion of renewable energy and ecosystem protection in Brazil and other ecologically sensitive regions.

SUMMARY

Brazil is especially relevant for tackling climate change while halting biodiversity loss due to its extensive areas of ecological significance, such as the Amazon rainforest. Addressing the issue between land-use demand for renewable energy development and protection of conservation land is key to aligning climate and conservation goals. However, the country's potential to achieve deep decarbonization through rapid renewable energy expansion while preserving conservation land remains underexplored. Here, we leverage a spatially explicit model through integrated, high-resolution sector coupling of Brazil's energy systems and find that doubling biofuel use by 2050 demands substantial land, primarily from degraded pastures. Strategic coordination of wind, solar, and biofuels can achieve deep decarbonization, cutting CO_2 emissions by 40%–91% while minimizing land competition and increasing system costs by less than 4%. Protecting these lands also facilitates reforestation, potentially sequestering an additional 15.43 Gt of carbon, demonstrating a viable synergy between climate mitigation and ecological integrity.

INTRODUCTION

There is a growing risk that energy transition conflicts with other UN Sustainable Development Goals (SDGs), such as SDG 15 (life on land), SDG 14 (life below water), and SDG 6 (clean water and sanitation).[1] In particular, large-scale land requirements for bioenergy crops[2] and renewable energy (RE) technologies[3,4] can drive ecosystem loss and degradation. This is particularly acute in Brazil, which is by far the most biodiverse country in the world[5] and therefore plays a key role in both preserving biodiversity and enabling effective climate mitigation through its energy and land-use strategies.

Brazil's long-term commitments include climate neutrality by 2050[6] and using biofuels as vectors for decarbonization and development, supported by the RenovaBio program launched in 2020. However, these long-term goals fail to provide guidance for spatial planning. By pushing new crops and pastures onto native lands,[7] they risk worsening issues related to food security,

land conflict, biodiversity,[2,8] and deforestation, particularly in the Cerrado savanna and Amazon rainforest. The problem also extends to wind and solar farms, which require large spacing areas and have already led to conflicts with local communities.[9] Furthermore, several wind parks have been deployed in priority areas for biodiversity conservation,[10] which, despite their importance in supporting ecosystem services, remain unprotected and vulnerable to human activities that might lead to land conversion and fragmentation.[11]

From the energy system perspective, a massive expansion and penetration of RE also leads to operational questions related to balancing variable generation and demand. Energy systems models with high temporal and spatial resolution can design technically feasible RE supply systems,[12] usually by performing cost minimization. Previous research has advanced in exploring long-term energy transition pathways using these models. For instance, detailed technoeconomic studies indicate that RE can meet Brazil's long-term demand at competitive costs.[13,14] In the biofuel sector, an analysis using optimization methods suggests that land-neutral methanol production offers carbon dioxide (CO_2) abatement costs comparable to those of other mitigation strategies, with production potential reaching nearly 50% of Brazil's current sugarcane ethanol output.[8] Another approach involves the use of integrated assessment models (IAMs), which provide a broader, cross-sectoral perspective by incorporating interactions between land use, energy, agriculture, and climate systems (e.g., BLUES for the Brazilian context). Findings from a study using BLUES demonstrate that preserving forests and restoring native vegetation are not only more cost effective but also more impactful mitigation strategies compared to relying solely on advanced technological solutions within the energy sector.[15]

Despite advances in understanding RE deployment and land-use dynamics, it remains unclear whether Brazil can meet its climate targets without increasing pressure on ecologically sensitive areas, particularly when long-term sector coupling is modeled. Furthermore, the long-term implications of alternative decarbonization pathways at high temporal and spatial resolution remain underexplored, both in technical terms (e.g., capacity expansion in highly electrified systems, operational strategies, storage requirements, and dispatch) and in terms of land-use conflicts and associated costs. This gap persists because existing studies often address energy systems in isolation, and those that attempt to integrate them typically rely on significant simplifications.[16,17] Clarifying these interactions is particularly urgent as Brazil expands biofuel production under the RenovaBio program and moves toward its 2050 net-zero commitment.[6] As infrastructure decisions made today will shape long-term outcomes, there is a timely need for integrated evidence on how to align decarbonization strategies with land conservation and broader SDGs.

Here, to fill these gaps, we develop a spatially explicit energy system framework with a high temporal and spatial resolution. The model integrates land-use constraints, including conservation-priority areas, Indigenous territories, and protected zones, into a national capacity expansion model for Brazil. The framework evaluates 16 policy-and-demand scenarios for 2050, quantifying trade-offs between decarbonization pathways, land use, and system costs. The results demonstrate that Brazil can reduce emissions from the energy sector without sacrificing priority lands for conservation or substantially increasing the costs of production. Findings also reveal where biofuel expansion risks land conflict (mainly with pasture and soybean production). Further, retaining conservation-priority zones in the "no-build" set allows their strategic reforestation to generate a significant carbon stock and land restoration. As the speed of energy system transformation increases at the same time as the urgency to preserve the biosphere grows, it provides insights for policymakers into sustainably achieving long-term decarbonization simultaneous with other SDGs, which could also be incorporated in future research.

RESULTS

Methods summary

We build two complementary energy-system models for Brazil in Calliope, which co-optimizes long-term capacity expansion and dispatch (Figure 1A). The first model component assesses bioenergy, considering suitable lands for feedstocks and their seasonality, conversion technologies, storage, and transportation costs. The second model component depicts the energy sector, including the expansion of mature technologies. Across both models, we focus on scenarios for different degrees of electrification (adding to the current electricity demand[18]) combined with policies of land use (preventing the use of conservation-relevant lands for energy purposes) and fossil-fuel phaseout (enforcing 100% RE supply), as well as the combination of both these policies (Figure 1B). Our approach permits us to show how much land is needed for bioenergy crops and energy-related infrastructure in 76 zones (Figure 1C) and where this infrastructure should be located, as well as the resulting costs and land-use impacts. Comparing scenarios with and without land-use restrictions permits us to investigate the potential for negative land-use emissions by shifting energy infrastructure away from conservation-relevant lands (Figure 1D) to preserve and restore them. For that, we calculate the potential contribution of reforestation by using a carbon stock difference approach.

Brazil-Calliope is made available online and fully reusable for further study of Brazil or other countries. Our results include multiple years of bias-corrected wind and solar data covering all of Brazil, as well as extensive georeferenced data, all of which can be freely reused.

Renewables meet high electrified demand with land limits

The cost-minimizing energy system model was designed to provide an energy supply system for Brazil that meets all demands for energy across the industry, transport, building, and agriculture sectors. We consider the spatiotemporal variability of renewable supply and energy demand resolved to 76 model regions within Brazil with a 3-hourly resolution. The model is run for all combinations of scenarios and policies, resulting in 16 system configurations. In all cases, power generation relies mainly on RE (Figure 2A). Detailed generation results are provided in Table S1. In the baseline scenario with default, 100% RE, and land-constrained (LC) policies, the system requires 394–398 GW of installed power generation capacity, 92%–100% of which is RE technologies. With high levels of electrification in the

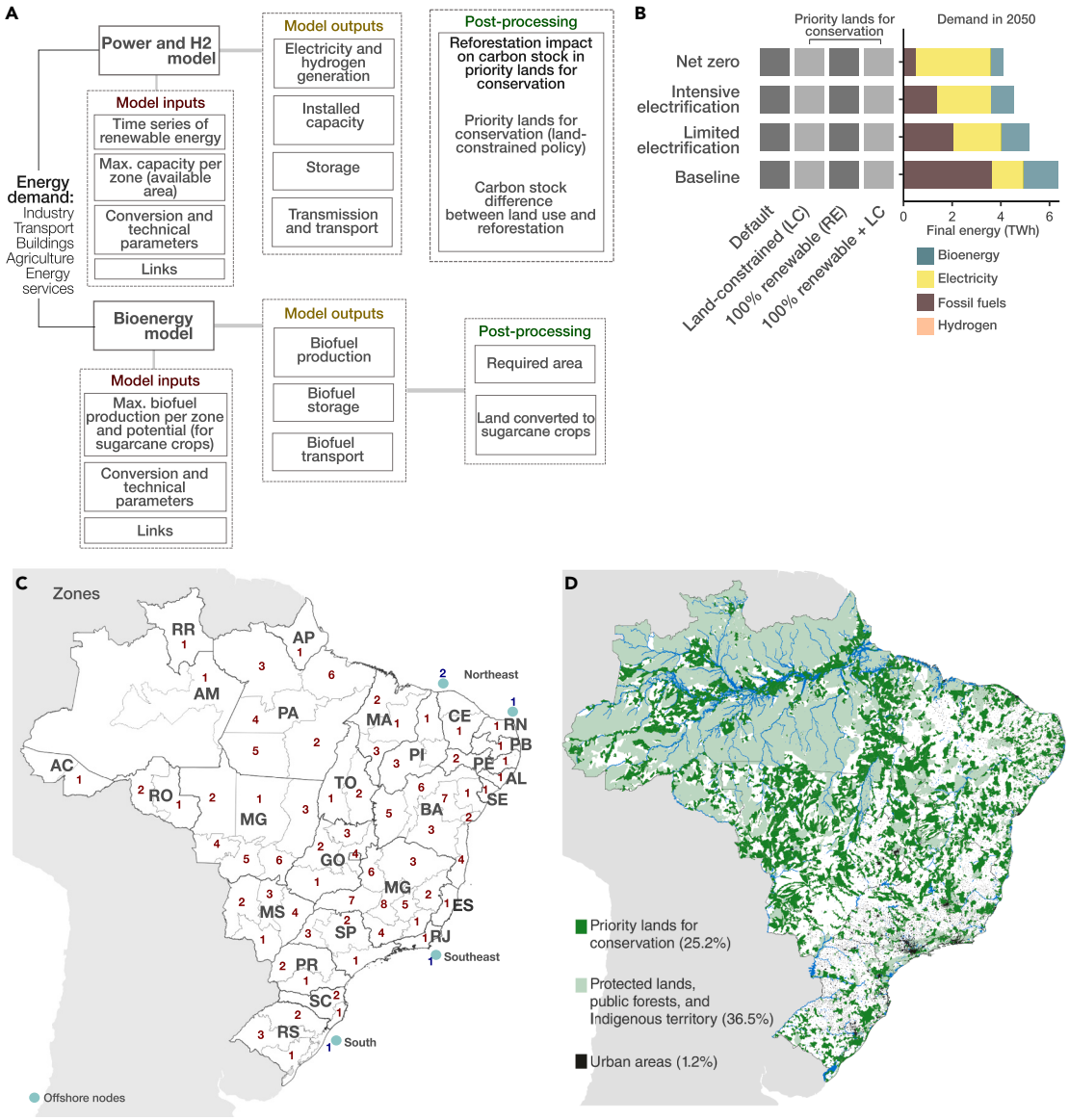

Figure 1. Overview of the modeling framework and spatial representation of Brazil's energy and land systems

(A) The workflow indicates the inputs, outputs, and post-processing stages, such as the required area calculations, land-use conversion analysis, and carbon stock potential of reforestation in priority lands for conservation.

(B) Scenarios for energy demand and energy system transformation (*y* axis) and the policies for land use and renewable energy deployment (*x* axis). Each square of the resulting scenario-policy matrix is assessed in our multi-model approach. The plot on the right represents the total final demand for fossil fuels, electricity, bioenergy, and hydrogen.

(C) Seventy-six zones of the Brazil power system model. The two-letter state abbreviations (gray) and the numbers (red) refer to the zones belonging to each state. Four of the zones, represented by light blue dots, are the regions considered for offshore wind energy. The name (gray) is related to the region and the number to the zones of each region.

(D) Overview of existing protected lands (light green) and additional priority lands for conservation, which are removed from consideration for energy infrastructure or bioenergy in the land-constrained (LC) policies.

net-zero scenario, Brazil would need more than three times the installed capacity of the baseline, with the cost-optimal configuration consisting of 43% wind energy and 24% solar energy (although we know from studies elsewhere[19] using near-optimal algorithms that it is possible to find solutions with very different wind and solar shares with a small cost increase). To put this into context, in the cost-optimal solution for the net-zero scenario, our most ambitious case, Brazil would deploy roughly 633 GW of onshore wind capacity, or 7.5 GW per 100,000 km^2 of land surface. This is less than half the current capacity density of Germany, which has roughly 60 GW of onshore wind capacity as of 2023, that is, 17 GW per 100,000 km^2 of land surface, although the nature and extent of land-use conflicts may differ substantially between countries.

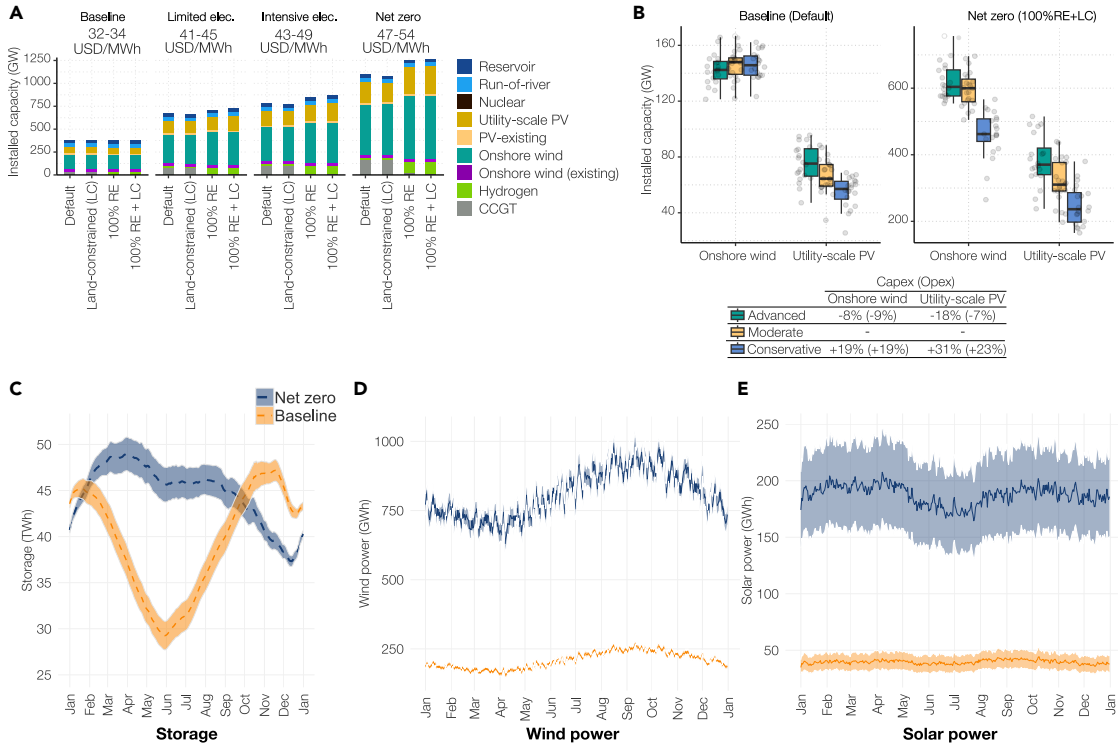

Figure 2. System capacity and renewable generation dynamics under different cost and policy assumptions

(A) Installed capacity in the reference weather year of four scenarios and four policies. The numbers above the bars indicate the range of levelized costs of electricity in every scenario for the moderate case and the representative year 2017.

(B) Boxplots of installed capacity in the baseline (default) and net-zero (100% RE + LC) scenarios for three cases of costs: advanced, moderate, and conservative. The light gray markers are the results across the weather years (2000–2019). The capex and opex (in parentheses) variations compared to the moderate case are indicated below the boxplot.

(C) The dashed lines indicate the daily hydro storage over the reference year of baseline default (yellow) and net-zero 100% RE + LC (blue). All other results of different weather years are in the transparent area.

(D) Wind power production over the reference year (dashed line) in the baseline default (yellow) and net-zero 100% RE + LC (blue) and other results of different years (transparent area).

(E) Solar power production over the reference year (dashed line) in the baseline default (yellow) and net zero 100% RE + LC (blue) and other results of different years (transparent area).

Due to the larger capacity required in high-electrification scenarios, the levelized costs of electricity increase by 30%, 40%, and 53% in limited electrification, intensive electrification, and net-zero scenarios, respectively, compared to the baseline.

We perform two sensitivity analyses: first, running the baseline scenario with both the default and the net-zero policies with 100% RE + LC across 20 weather years (2000–2019), and second, varying the capital expenditure (capex) and operating expenses (opex) of onshore wind and utility-scale photovoltaic (PV) technologies based on the conservative, moderate, and advanced cases of the National Renewable Energy Laboratory (NREL).[20] The weather year 2017 is the reference, and all results refer to it unless otherwise indicated. The weather sensitivity analysis shows that the standard deviation of installed capacity in the net-zero scenario is higher than in the baseline scenario, indicating that large renewable systems are more vulnerable to weather conditions. The cost sensitivity analysis indicates that the moderate case of wind farm costs resulted in larger wind capacity than the advanced case (lower costs), where we observed an increase in solar farm capacity (Figure 2B).

We find that hydro reservoirs (145 TWh of maximal storage capacity) remain the main electricity storage system. Their dispatch changes with the addition of large-capacity wind farms in the net-zero scenario (Figure 2C). In the dry season (from June to September[21]), wind power output is usually larger than in the rainy season, implying a reduction in hydro dispatch (Figures 2D and 2E). However, the system consumes much of the available hydropower potential during the rainy season, when demand is higher and wind potential is lower, implying less storage of hydropower reserves. Dispatchable natural-gas-fired power plants are still part of the solution for peak hours, particularly during the rainy season (summer) in the baseline scenario. However, in 100% RE cases, natural gas is completely replaced by RE, including green hydrogen as storage, which is then converted back to electricity through hydrogen combustion.

Electrification pathways require more power infrastructure land than the baseline scenario, excluding the bioenergy-dedicated lands. The estimated footprint for power generation infrastructure, which in our accounting includes the turbine spacing area for wind farms, increases from approximately 42,648 km^2 in the baseline to 158,410 km^2 in the net-zero default scenario

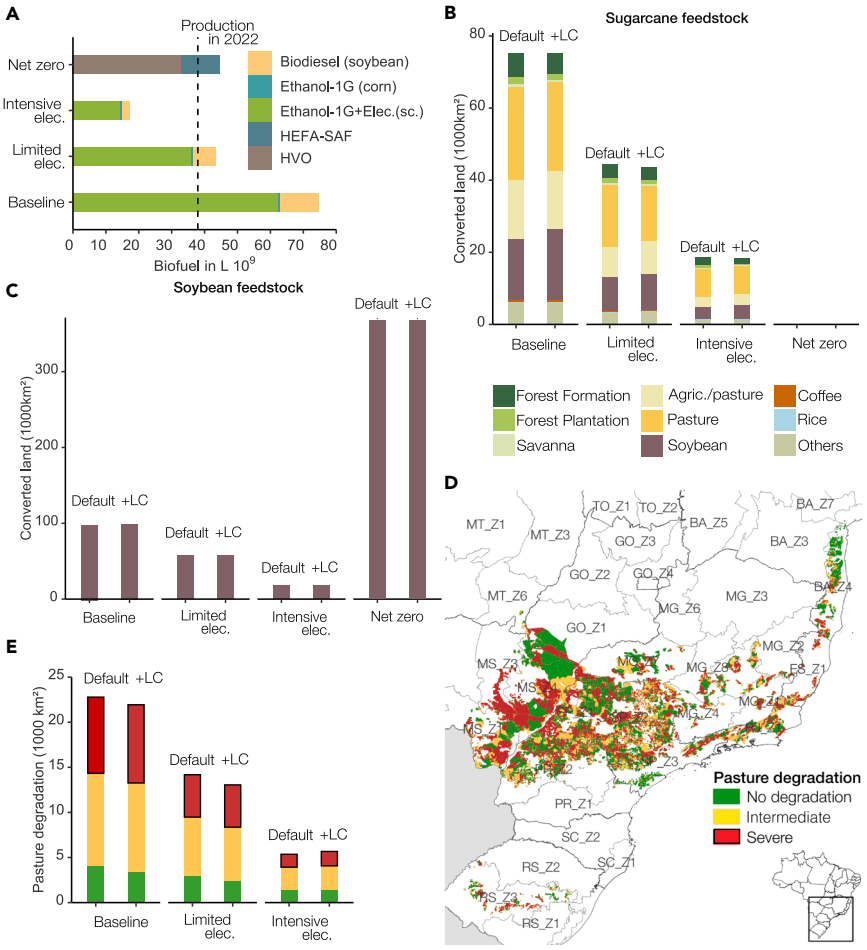

Figure 3. Biofuel production and land conversion under different scenarios

(A) Production of liquid biofuels in four scenarios: baseline, gradual electrification, intensive electrification, and net zero. The biofuel production is the same for both default and land-constrained (+LC) policies. The dashed line indicates today's production (37.9 billion liters). sc. represents ethanol from sugarcane.

(B) Total dedicated land area in square kilometers to produce liquid biofuels from soybeans in four scenarios. The total converted land is the same for default and +LC policies.

(C) Land conversion to sugarcane crops to produce ethanol. Default indicates that there is no policy, while +LC represents the land-constrained policy (the use of priority lands for conservation is not allowed for energy purposes).

(D) Level of pasture degradation (severe, intermediate, and no degradation) in areas with high potential for sugarcane crops.

(E) Converted area of pasture to sugarcane crops in four scenarios with default and +LC.

(199,353 km^2 in the 100% RE scenario). In this category, wind farms account for 98%–99% of the area, because turbine spacing dominates the spatial extent (see Table S2 for further details). This footprint is reported separate from the land physically converted for bioenergy feedstock cultivation.

Biofuel production sparks land-use conflicts

The bioenergy model includes 72 zones and five carriers: ethanol from sugarcane (first and second generation), first-generation ethanol from corn, biodiesel and hydrotreated vegetable oil (HVO) from soybean, sustainable aviation fuel (SAF) from ethanol and soybean, and charcoal. In our model we limit land availability for sugarcane crops to the Agroecological Zoning of Sugarcane (revoked decree that established spatial planning for sugarcane crop expansion),[22] that for corn exclusively to existing off-season crops (where corn is grown outside of the typical growing season), and that for soybean to existing soybean crop areas. Charcoal's potential is given by existing silviculture activity.[23] We run the bioenergy model for all scenario combinations, considering both the default and the LC policy, using a 120-h resolution. This resolution is appropriate given the slower dynamics of bioenergy systems, such as crop seasonality, biomass processing, and storage constraints. Unlike power systems, where RE fluctuations necessitate a finer temporal resolution to capture short-term variability, bioenergy production operates on longer timescales, making the model computationally feasible.

Liquid biofuel production reaches 74.7 billion liters in the baseline scenario, almost double the current production, but decreases to 43.3–17.2 billion in the electrification scenarios (Figure 3A). Fossil fuels still represent 57%, 39%, and 30% in baseline, limited, and intensive electrification scenarios. First-generation ethanol is still relevant in the intensive electrification scenario, particularly for the industry sector (food and beverage, ceramic, cement, etc.). However, in the net-zero scenario, which assumes near-complete electrification, the demand for ethanol is completely replaced by electricity. We assume instead that the demand for hard-to-electrify transport subsectors (aviation, shipping, and long-distance road freight) is met by 44.6 billion liters of HVO and SAF, eliminating fossil fuels for the transport sector. To see the detailed biofuel demand for each subsector see the supplemental information.

We consider two technologies for SAF production; however, we assume the least-cost option, hydroprocessed esters and fatty acids (HEFA) plants with soybean oil as feedstock, is used for SAF production. For HVO, we consider its production exclusively from soybean and its existing crops. Due to the lower yield of soy crops compared to sugarcane, the net-zero scenario requires more land than other scenarios: 360,000 km^2 compared to around 20,000–200,000 km^2 of dedicated land in the other three scenarios (Figure 3B). The required areas and biofuel production are summarized in Table S3.

Charcoal rises to 9.8 Mt (baseline) and drops to 8.9 Mt (electrification and net zero) due to the electrification of the building and agriculture sectors. Still, the production of charcoal exceeds current levels by 44% (baseline) and 31% (electrification, net zero), primarily due to its use in heavy industry (pig-iron steel and cement).

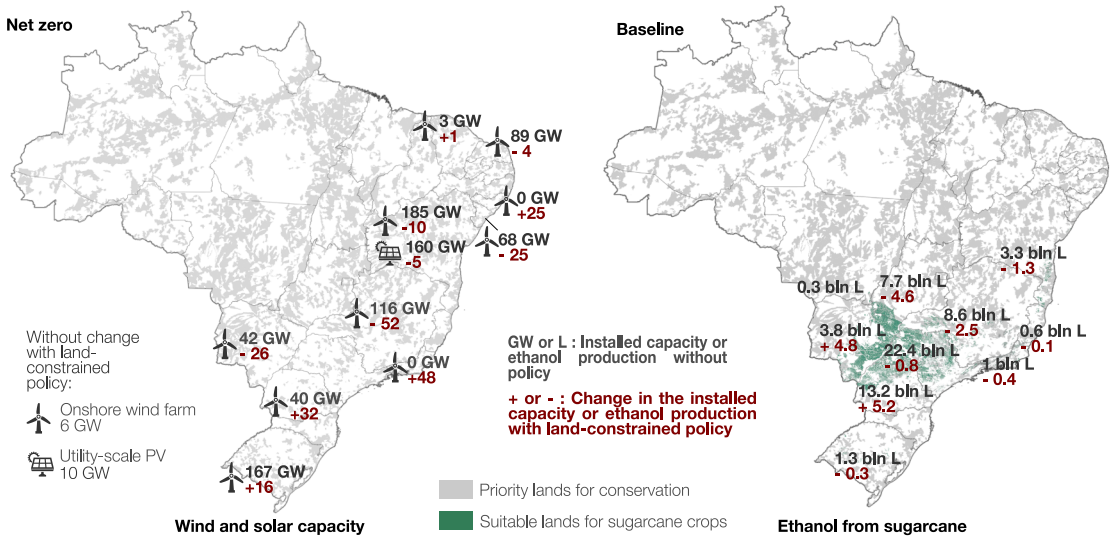

Figure 4. Spatial shifts in renewable generation and biofuel production under land-constrained policies

Shifts in the installed capacity of wind and solar farms (left) and in ethanol production (right) when land-constrained policy is considered. The first map represents the changes in the net-zero scenario, and the second one indicates the changes in the baseline scenario.

Sugarcane remains the primary feedstock for ethanol production, and utilizing bagasse for electricity combined with storage systems is more viable than second-generation ethanol in our work (see Figure S1 for electricity in the co-generation process). To avoid food conflict, we assume that corn-based ethanol expansion beyond the current production is not possible, as it requires almost twice the land to produce a liter compared to sugarcane. Corn-based ethanol reached its maximum production in all scenarios (0.67 billion liters).

We limit the production of soybean to existing soy crop areas, but allow for expanding sugarcane to produce ethanol on additional potential lands (classified into high, medium, and low potential cultivation areas). This means that the land may currently be used for something other than sugarcane. Resulting from this, we find a large area conversion from pasture, a mosaic of agriculture and pasture, and soybean to sugarcane crops (Figure 3C). Lands dedicated to sugarcane conflict with 754–4,629 km^2 of food production (excluding livestock and soybean crops), being larger in the baseline scenarios and representing 3.9%–5.5% of the required land (see Table S4).

While sugarcane crops compete with other uses, results show that land management can reduce the conflicts. For example, 67%–81% of pasture lands converted to sugarcane crops are degraded pastures (Figures 3D and 3E), which could have higher livestock productivity through their recovery, occupying a smaller area. Despite our findings, we observe that there are available lands with high potential for sugarcane (over 23,000 km^2 in Mato Grosso do Sul) that are not part of our optimal results, but with appropriate land management, these areas could potentially alleviate the pressure on food production lands. For soybean land conflict, adopting available and future technologies and using further degraded pastures are additional opportunities for production increase. Moreover, there are techniques such as biological nitrogen fixation, no-tillage farming, and integrated management of pests and diseases that,[24] although well known in Brazil, remain underutilized on a national scale.

Sensitivity analysis: Ethanol-to-e-methanol pathway (alternative net-zero scenario)

In a sensitivity analysis, the alternative net-zero pathway, meeting 50% of the long-term demand for light-duty vehicles through sugarcane-based ethanol production, results in approximately 26.7 million tonnes (Mt) of biogenic CO_2 emissions, derived from fermenting 35.7 billion liters of ethanol. Capturing this biogenic CO_2 presents an opportunity to synthesize around 24.6 billion liters of e-methanol. This volume of e-methanol could replace 34.15% of the projected demand for HVO in the original net-zero scenario, particularly supplying the shipping and long-distance trucking sectors.

Producing this amount of e-methanol needs about 3.65 Mt of green hydrogen, which, in turn, requires 204.44 TWh of renewable electricity. The majority of this energy demand stems from the electrolysis process used to generate H_2, highlighting the importance of expanding Brazil's RE capacity. To put this into context, the electricity required exclusively for the electrolyzer represents 7.3% of the total electricity demand in the alternative net-zero scenario. This total demand, which includes both system demand and the electricity required for hydrogen production used in e-methanol synthesis, is comparable to the total electricity demand in the original net-zero scenario, where 100% of light-duty vehicles are electrified. Further analysis is needed to determine the optimal installed capacity and its spatial distribution.

By producing e-methanol, the land required for soybean cultivation decreases from 360,000 to 122,400 km^2. However, this is partially offset by an increase of 48,572 km^2 in sugarcane area, resulting in a total land use of 170,972 km^2. Table S5 details the land conversion through the expansion of sugarcane cultivation in the alternative net-zero scenario.

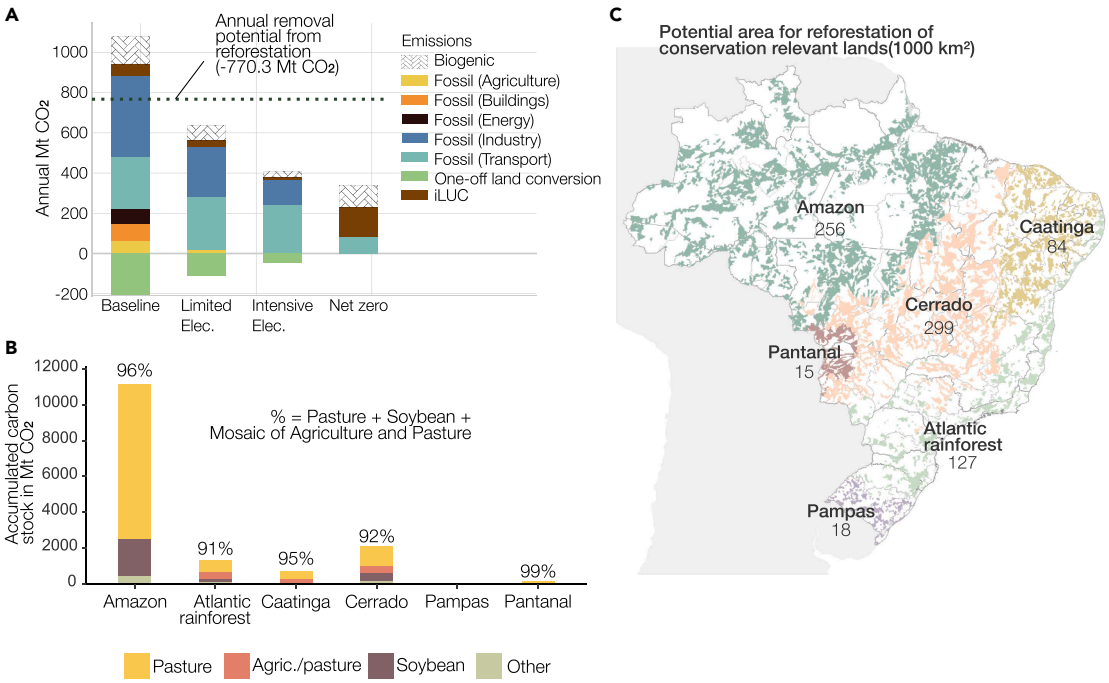

Figure 5. Emission balance and reforestation potential

(A) Fuel combustion emissions from the agriculture, building, industry, and transport sectors and energy services; one-off land conversion emissions related to the biofuel-dedicated lands; and annual iLUC emissions in the 100% RE and land-constrained scenarios (except life-cycle emissions). Hatched bars indicate biogenic emissions. The dashed line indicates the potential annual CO_2 removal from reforestation and should be interpreted as a negative value.

(B) Accumulated carbon stock potential of six biomes from recovering 100% of priority lands for conservation. The percentage above the bars indicates the share of land use that is pasture, soybean, and mosaic of agriculture and pasture. The absorption is for the area highlighted in (C).

(C) Potential area for reforestation by biome, considering the total area of priority lands for conservation. The number below the biome's name represents the total area of proposed recovery in 1,000 km^2.

Land conservation adds minimal energy cost

The LC and 100% RE + LC policies entirely prevent the use of lands with priority conservation status for energy purposes. This shifts the deployment of wind and PV capacity or bioenergy crops to different locations. The power system configuration remains entirely unchanged when introducing land constraints into the baseline scenario, as sufficient land remains available at the most optimal deployment locations. On the other hand, we observe significant changes in where renewable electricity generation is deployed in the electrification and net-zero scenarios. For biofuels, the largest shifts of bioenergy crops occur when imposing land constraints in the baseline scenario, which has the largest ethanol demand. Sugarcane crops for ethanol production move into a new arrangement, with a reduction of crops in the southeast and an increase of crops in the midwest (Mato Grosso do Sul), south (Paraná), and northeast. Figure 4 shows the main changes in wind and solar capacity in the net-zero scenario and ethanol production in the baseline scenario.

We find that preserving priority land for conservation has no cost effect in the baseline and only a minimal additional cost in more electrified scenarios, ranging from 0.1% to 4% of the total levelized costs without LC policy, even with significant shifts of optimal locations. For sugarcane crops dedicated to ethanol production, we observed that the total costs remain unchanged with the land shifts. This further suggests that many near-optimal alternative solutions exist and shows that a completely RE system can co-exist with a strong land conservation policy.

Managing land and energy drives emission cuts

The baseline scenario has substantial emissions, reaching 887 $MtCO_{2equiv}$ from fossil fuel combustion and an additional 137 $MtCO_{2equiv}$ from biogenic emissions (Figure 5A), referring to the CO_2 released when recently grown biomass is burned or digested. As the scenarios progressively shift toward electrification, the emissions decline. In the net-zero scenario, the emissions fall by 91%, compared to the baseline (without biogenic emissions), to 79 $MtCO_{2equiv}$. The remaining emissions come from cement, chemical, and metallurgical industries, which our model assumes cannot be decarbonized (possible solutions such as carbon capture and storage [CCS] are not considered).

The carbon stock balance from land conversion to sugarcane crops is positive, as many converted lands are currently degraded pasture. The CO_2 removal varies according to the demand for ethanol (Figure S2), being larger in the baseline scenarios (174–223 $MtCO_2$) and lower in the electrification scenarios (21–119 $MtCO_2$). See Table S6 and Figure S3 for the alternative net-zero scenario. Scenarios with the default policy have lower CO_2 absorption than the LC policy, in which removals increase by 21–48 $MtCO_2$. This is because with the LC policy, we avoid land use for energy purposes in areas with larger carbon stock. Emissions due to land conversion for the production

of HVO, SAF, corn-based ethanol, and biodiesel are considered inexistent, as we restrict their feedstock production to existing cropland areas and thus assume no changes in the land-use class.

The estimation of indirect land-use change (iLUC) emissions varies depending on the method used. For soybean-based biofuels, we consider a range of values derived from different methods. In the baseline scenario, iLUC emissions range from 36 to 75 $MtCO_{2equiv}$. Under limited and intensive electrification scenarios, these values are reduced by 42% to 80%, respectively (Table S7). However, in the net-zero scenario, iLUC emissions increase significantly, ranging from 80 to 214 $MtCO_{2equiv}$, due to the high demand for biofuels in hard-to-electrify sectors.

We find that land management toward land recovery and reforestation in conservation-relevant lands could further help mitigate climate change and potentially neutralize the remainder emissions from hard-to-electrify subsectors. When lands are freed up from energy use in scenarios with the LC policy, the potential CO_2 sequestration due to reforestation is high. A total of 15,430 $MtCO_{2equiv}$ additional carbon stored is possible (Figure 5B), without considering possible losses due to wildfires. The Amazon rainforest contributes to 72% of the potential, followed by the Cerrado, which has an additional carbon stock of 2,090 $MtCO_{2equiv}$ and contains the largest area of priority lands for conservation (Figure 5C). Apart from the carbon stored, the annual CO_2 absorption is slightly higher in the Cerrado (386 $MtCO_{2equiv}$ $year^{-1}$) than in the Amazon (314 $MtCO_{2equiv}$ $year^{-1}$). Table S8 shows the annual removal by biome after reforestation.

Most of the land proposed for reforestation is currently used for pasture and soybean production in all biomes (91%–99%), while food production (excluding beef) represents 0.98%. There is a potential for better land management, particularly of pastures, but the high dependency on soy-based biofuel in the net-zero scenario may itself lead to significant land conflicts.

Although we report the total carbon stock, that pool accumulates gradually over time. Growth rates differ by biome, with peak sequestration around year 2025 before declining.[25] Thus, the strongest climate-mitigation impact of reforestation arrives a few decades after implementation.

DISCUSSION

We find that optimal energy systems rely mainly on RE, even in highly electrified systems. In our scenarios, onshore wind is the predominant source of clean electricity, followed by centralized solar generation, regardless of the policy considered. Offshore wind farms were not assumed to be cost competitive in our work, but based on work elsewhere in the world,[19] it is reasonable to assume that, looking for near-optimal alternative energy system configurations, systems with high shares of offshore wind would be equally feasible. The power system transition and expansion are expected to increase significantly in highly electrified scenarios. Statements about the total investment are not possible in our work, since the costs refer exclusively to the capacity expansion and do not account for expenses related to transmission infrastructure, charging stations, industrial adaptation, and other necessary components for a highly electrified system. Additional research is necessary to investigate these issues.

The demand for biofuels in 2050 is significant for both the net-zero (HVO and SAF) and the baseline scenarios (mainly ethanol), exceeding the current level of biofuel production. Crops for biofuels need significant direct land use, leading to land conversion, impacting particularly existing pastures and soybean crops in baseline and electrification scenarios. Land conversion leads to considerable iLUC emissions in both the baseline and the net-zero scenarios. In the latter, emissions rise significantly due to the intensive use of soybean as a feedstock to decarbonize hard-to-electrify sectors. These values should be treated as indicative of the range of potential impact due to the high level of uncertainty. A deeper analysis of converted pasture lands reveals they are primarily degraded pastures, suggesting potential positive outcomes through transitions to sugarcane crops and increased ecosystem services, as also confirmed in another study.[26] Biofuels in the net-zero case are fully based on soybean feedstock, requiring a land area equivalent to 49% of Brazil's current soybean land (360,000 km^2).[27] With a substantial portion of current soybean production being dedicated to animal feed (76%[28]), further land expansion may occur to meet energy and non-energy feedstock demand.

Without significant worldwide dietary shifts and land management, Brazil risks facing land conflicts and deforestation. Diversifying feedstocks could help alleviate the land conflict associated with biofuel production, although it may not completely eliminate land stress. We consider only national demand for energy; however, the demand for biofuels may be considerably higher if they are traded internationally.

The required area for the expansion of the energy system, particularly for biofuels, is significant. Restricting the energy-related use of priority lands for conservation impacts the energy system's configuration and feedstock crops' location. Findings show that the LC policy is a strategic way to mitigate biodiversity loss, resulting in no significant difference in energy costs compared to cases without land restriction. Even in the more electrified scenarios, where optimal locations may undergo substantial shifts, the cost increase does not surpass 4% beyond the optimal cost. However, these costs represent the levelized cost of energy without considering the reallocation of transmission expansion, for instance. Accordingly, the reallocation without significant change in costs should be viewed strictly as generation-level costs, not as systemwide totals. Nonetheless, historical data from Brazil's national energy plans suggest that transmission capex typically comprises only 5%–10% of total energy-sector investment.[29] Given this relatively small share, the additional expansion required to accommodate infrastructure reallocation under conservation-priority land restrictions is likely to have a limited impact on overall system costs.

Given the considerable uncertainties in future technology costs, this can be considered an insignificant increase and essentially the same cost as the cost-optimal configuration. Past work using modeling to generate alternatives (MGA) methods has considered a cost increase of even 10% acceptable.[30]

Another point of attention is water use, which we ignore in our model. Although sugarcane crops for ethanol production are shifted to regions with a well-developed agribusiness sector, the water conflict between consumptive uses is a drawback, particularly in the northeast region, where irrigation is necessary

in an area regularly suffering from droughts.[31,32] See Figure S4 and Table S9 for details on irrigation needed for sugarcane-based ethanol.

Regardless of the LC policy, our findings indicate that emissions can almost double the current levels if no significant changes are made in the energy transition. In the net-zero scenario, emissions from fuel combustion decreased by 91% compared to the baseline but still had a remainder associated with heavy industries. Although not included in this work, CCS has been discussed as an alternative for net-zero pathways in industry.[33] However, in Brazil, a commercial scale of CCS can take another 12 years and cost USD 305/tCO_2.[34]

Bioenergy is essential to reduce emissions in sectors where electrification is difficult (e.g., aviation, maritime, and long-distance road transportation). Its biogenic emissions are absorbed by the plants grown in a carbon-neutral cycle. Still, reforestation in conservation-relevant lands has a huge potential for carbon sequestration (16 times the emissions in the baseline scenario). However, while burning emissions are instantaneous, removals by the natural cycle might take a long time.[35] Such lags in resequestrating carbon might negatively impact rapid decarbonization.

Our analysis explores technically and environmentally feasible energy transition pathways for Brazil while recognizing that certain aspects remain beyond its current scope. The study assumes a strong role for biofuels in decarbonizing hard-to-electrify sectors and excludes large-scale deployment of CCS. Political and institutional dynamics—such as lobbying influences and employment dependencies within the ethanol sector—were not explicitly modeled but may shape the real-world implementation of the technically optimal pathways identified here. Similarly, transmission costs, pipeline infrastructure, and emissions from wildfires and industrial processes were not included due to data limitations.

Nevertheless, our results make a clear case for the possibility of achieving deep decarbonization by 2050 while protecting and restoring conservation-relevant land, all while building on Brazil's strengths of natural resources (abundant hydropower, bioenergy potential, and wind and solar resources). Brazil's Nationally Determined Contributions (NDCs) and the SDGs are synergistic. For example, restoring ecological lands can reduce emissions and preserve biodiversity (SDG 15). Yet, reforestation alone is insufficient, since a transition to clean energy is essential to avoid local pollution and support sustainable cities and communities (SDG 11). Careful spatial planning will help minimize environmental impact and conflicts and should also be conducted for "low-land-footprint technologies" like wind farms, since their necessary support infrastructure might still affect ecological corridors and natural habitats. Also, although our analysis excludes areas of environmental conservation, the remaining land should not be interpreted as unoccupied or free from potential conflict. Many of these areas are known to be inhabited or used by traditional communities (e.g., quilombolas), which are vulnerable to large-scale infrastructure deployment. The problem of large-scale appropriation of public lands for RE development has already been highlighted in past work.[36] Further research is needed to better understand and incorporate these dynamics, particularly given the limited availability of data on these communities' occupations in Brazil.

Finally, addressing climate change and halting biodiversity loss have become an urgent issue involving all societal levels. Brazil has the potential to become a major player in the fight against climate change and ecological degradation if policy is designed accordingly.

METHODS

We developed the Brazilian energy model using Calliope and analyzed four scenarios: baseline, limited electrification, intensive electrification, and net zero. Then, we explored these scenarios under land conservation and 100% renewable system policies. Finally, we proposed the recovery of conservation-relevant lands to estimate their contribution to carbon storage (Figure S5).

We prepared the model inputs in a pre-processing step that included spatial analysis (land availability), time series of renewable resources and demand, and scenario definition. As the final results from the model, we obtained the energy system configurations across multiple scenarios and weather years. Besides the energy-related results, we discussed further implications on converted lands and greenhouse gas (GHG) emissions.

Energy system models

We built the Brazilian energy model using Calliope, an open-source, linear optimization-based energy modeling tool with the default objective function of minimizing total system cost or emissions while meeting all energy demands according to Equation 1,

$$\min z = \sum_{loc::tech_{cost}k} (cost(loc :: tech, cost = cost_k)) + \sum_{loc::carrier,timestep} (unmet\_demand(loc :: carrier, timestep) \cdot bigM), \quad \text{(Equation 1)}$$

where k is associated with the costs of each technology (tech) and location (loc). Unmet demand is multiplied by *bigM*, a large positive constant representing an upper bound or an infinite value in mathematical models.[37] For more details, see Figure S6.

Calliope is flexible and appropriate for highly renewable systems, since the framework can incorporate resource fluctuations through time series and spatial nodes. However, large energy models usually suffer from high computational costs. Due to our extensive scope, we split the model into two parts (the bioenergy model and the power and hydrogen model) that can be run independently (see Figure S7). With that, we kept the computational complexity manageable and increased accessibility to further research without necessarily depending on high-performance computing (HPC). We used the solver Gurobi.[38]

With the bioenergy model, we investigated liquid and solid biofuels. The power and hydrogen model explored two other carriers: electricity and hydrogen. Electricity in the bioenergy model is an exclusive production from by-products. Part of its production is consumed at the refinery or distillery, and the surplus goes to the grid. The surplus power generation in the bioenergy model was then discounted from the demand of the energy model.

We included time series of demand and RE in the power model available at hourly resolution. We ran the scenarios of the energy model at a 3-hourly resolution on a DelftBlue high-performance computer.[39] The bioenergy model was run at a 120-hourly resolution.

Scenarios

We investigated four scenarios: baseline, limited electrification, extensive electrification, and net zero. The baseline represents the demand estimation for 2050 from the Brazilian Energy Research Office (EPE).[18] Based on this demand, we made assumptions about demand variations for electrification and net-zero scenarios using different carriers. To ensure logical and realistic assumptions, we considered electrification technologies that are already fully developed. However, there may be obstacles related to infrastructure or technical implementation that can potentially hinder the progress of electrification (e.g., the absence of charging stations for electric vehicles in remote regions, irrigation in rural areas not connected to the grid, etc.). Therefore, limited electrification considers these barriers and has a smaller share of electrification (even with available technology at a commercial scale); extensive electrification and net-zero scenarios assume barrier elimination and, consequently, a higher level of electricity demand. The detailed assumptions for every subsector are available in the supplemental information.

In this study, net zero refers exclusively to scenarios explicitly designed to reduce fossil fuel use in the energy sector to a level that is as low as technically and economically feasible, leaving only minimal residual emissions to be balanced. Scenarios with higher fossil-fuel reliance, even if their emissions could be offset by reforestation, are not classified as net zero, as our definition emphasizes direct decarbonization rather than achieving balance primarily through land-based removals.

Besides the exploratory demand scenarios, we analyzed them under four policies:

- Default: no new policy is implemented.
- LC: priority lands for conservation are preserved.
- 100% renewable power system (100% RE): the power system is transitioned to 100% RE.
- LC combined with 100% renewable power system (LC + 100% RE): priority lands for conservation are preserved, and the power system is transitioned to 100% RE simultaneously.

The net-zero pathway relied heavily on HVO, resulting in extensive land requirements for soybean cultivation. As a sensitivity analysis, we proposed an alternative pathway that uses biogenic CO_2 captured from the fermentation of sugarcane-based ethanol to produce e-methanol. We assumed that 50% of the light-duty vehicle fleet was electrified, while the remaining 50% continued to operate on ethanol (rather than 100% electrified). The outcomes are mainly presented in the supplemental information.

We analyzed the sensitivity of the power system capacity to weather years and cost variation. For the weather analysis, we investigated 20 years of wind, solar, and hydro resources and demand profiles. For the cost analysis, we considered three levels for wind, solar, and battery costs, conservative (higher costs), moderate, and advanced (lower costs), based on data published by the NREL.[20]

In this study, net zero refers to a state in which GHG emissions from the electricity and hydrogen sectors are reduced to the lowest technically and economically feasible level, with only residual emissions balanced by CO_2 removal from reforestation. This definition is sector specific and does not imply that the entire economy achieves net-zero emissions. Certain industrial subsectors, such as cement and chemical production, are expected to retain a degree of fossil-fuel dependence due to technological and economic constraints. Consequently, while the modeled net-zero pathway nearly eliminates fossil-fuel use in the energy sector, it co-exists with residual emissions from other sectors that are not addressed within the scope of this study.

Several pathways and technologies can be explored in scenarios. It is important to note, however, that our objective was not to forecast future demand. Instead, we analyzed different scenarios while considering specific constraints.

Land availability

Land availability is a key factor in determining the maximum available area for technologies or feedstocks that require large areas and could impact human activities or natural ecosystems.

We excluded lands protected by law, public forests,[11] rivers, lakes,[40] and Indigenous territory[11] in all scenarios and policies, as they have a well-known role in conservation and mitigating climate change.[41] For further details, see Figure S8A. We applied a buffer of 2 km around these areas.[42] We further excluded urban areas with a buffer of 0.5 km. This first criterion applied to all scenarios due to legal ineligibility for large-scale deployments. Then, for the LC policy, we excluded priority lands for conservation.[43] These lands are not currently protected by law, but they are conservation-relevant areas due to their high biodiversity importance. These areas maintain ecological services, such as carbon storage, water regulation, and nutrient cycling. The data are based on the systematic conservation planning (SCP) method[43] (see Figure S8B). Although they are an important instrument for spatial planning, many large-scale wind or solar parks have been built ignoring these lands. For existing parks, the exclusion of relevant ecological lands was not taken into consideration.

The land suitability for sugarcane crops was given by the Agroecological Zoning of Sugarcane (ZAE Cana, in Portuguese).[22] ZAE indicates the potential (high, medium, and low) of sugarcane crops according to the soil's physical, chemical, and mineralogical characteristics and weather conditions (Figure S8C). For corn-based ethanol, we considered its production only from existing off-season crops, where corn is grown outside of the typical growing season (Figure S8D). Soybean oil is the most commonly used feedstock for biodiesel[44] and HVO[45] production due to its high competitiveness compared to other oilseeds.[46] Charcoal is produced by existing silviculture activity given by Souza et al.[23]

Inconsistencies in defining and measuring land-use requirements (LURs) can lead to variations in reported values.[47] These differences come from methodological choices, such as whether the area is defined by infrastructure only or by spacing area or includes temporary and remote areas. Here, to estimate the land footprint of wind and solar farms, we considered the spacing

area from theoretical approaches. For wind energy, the calculation was based on reference turbines—Vestas V150 (4 MW) for onshore and Vestas V164 (8 MW) for offshore installations. The required area was determined using an average spacing of 10*D* by 5*D* along the *x* and *y* axes, respectively, where *D* is the rotor diameter.[48] For utility-scale PV systems, we applied a capacity area of 79 MWp/km^2, as reported by the EPE.[49] For the rooftop PV area, see the "solar power" section.

Zones and links

Although Brazil has interconnected transmission lines covering almost the entire territory, we created zones to include the heterogeneity of different regions (see Figure S9). We divided the Brazilian state territories into zones following two steps. The first was based on concession areas of power distribution companies (described in Table S10). With that, we had a more realistic demand per zone, making it possible to distinguish the share of electricity consumption in different economic activities and population levels. In states with many companies, particularly in the south and the southeast, we merged small concession areas to form a single zone. In some large states (e.g., Pará), where only single companies control distribution, we used mesoregion limits to determine zones and divided the state's demand by the zone's population. We excluded part of the Amazon region where the supply comes from isolated systems.

We established links between zones to make the carrier exchange possible. For electricity, we identified the nearest existing substations[50] to the centroid of each zone. Using the QGIS function "simplify vector," we simplified the existing and planned transmission lines.[50] We considered a general loss of 5% per distance between zones.

Today, ethanol transportation relies mainly on road transport for the internal market and shipping for exports. To calculate the road distance between zones, we estimated the shortest path through roads between the zone's centroids using the QGIS function "network analysis - shortest path." Costs per distance traveled by trucks were from Khatiwada et al.[51] Similarly, we created pipeline connections using the same road path and assumed the costs and parameters of an existing pipeline between Ribeirão Preto and Paulínia.[52]

Conversion technologies

For the bioenergy model, we considered five carriers: ethanol, HVO, biodiesel, SAF, and charcoal. We assumed two types of distillery for ethanol production that uses traditional sugarcane. The first is the conventional one, able to produce first-generation ethanol (from the juice) and generate electricity from the residuals (bagasse).[53] The second one produces both first- (juice) and second-generation ethanol (bagasse). For corn-based ethanol, we assumed a full distillery capable of processing only corn and producing first-generation ethanol.

Capex refers to refinery installation costs and opex to annual operational costs, both converted to USD/L (see Table S11 for detailed costs). Here, opex includes feedstock costs as well. For ethanol from sugarcane, we obtained the total refinery costs from Khatiwada et al.[51] and converted them to USD/L using the historical productivity data for first-generation ethanol.[54] We considered a conversion factor for second-generation ethanol production of 57% from first-generation ethanol for conventional sugarcane.[55] The capex includes the costs of first- and second-generation ethanol. For second-generation ethanol, we included enzyme expenses. We obtained capex and opex from the EPE[44] for corn-based ethanol. Agricultural costs of corn crops are from a typical farm located in Santa Catarina State.[56]

Although technologies that produce second-generation ethanol are more expensive, they become cheaper when the costs are in terms of liters, since they can produce more ethanol. In that sense, we set no costs for electricity generation and added a payment for it, since there is no demand for electricity in the bioenergy model. Based on the prices in auctions in 2022,[57] we considered the average price of USD 76.49/MWh and production of 1 MWh for every 3,800 L of ethanol produced. This results in USD 0.0134 per liter of ethanol if the refinery produces electricity from the bagasse.

The overall efficiency improvement happens through better distillery conversion and agricultural progress.[58] We considered an annual productivity increase of 0.9% for conventional sugarcane,[59] as our estimation was based on historical values, and many farms do not operate with cutting-edge technologies. We considered that the efficiency increase for ethanol from corn followed the same overall progress as traditional sugarcane. Still, we assumed that ethanol capex and opex would be reduced by 10% and 25%, respectively, by 2050.[60]

Table S12 shows the pipeline parameters adopted for ethanol transportation. We assumed parameters from an existing pipeline (Ribeirão Preto-Paulínia).[52]

Soybean oil is one of Brazil's most commonly used feedstocks for biodiesel and, consequently, a competitive feedstock option. Here, we considered soy oil as a feedstock to produce HVO and biodiesel in the long term. For SAF, we consider two types of refineries: hydrotreatment of soybean oil (HEFA) and dehydration and oligomerization of ethanol-alcohol-to-jet (ATJ technology). Estimated costs for SAF are from Capaz et al.,[61] for HVO from the Danish Energy Agency,[62] and for biodiesel from the EPE.[44]

About 80% of the charcoal production in Brazil is through low-tech kilns, which lack the control of gas emissions generated by carbonization.[63] Here, we considered a more technologically advanced system called Ondatec (microwave carbonization kiln) and the feedstock from *Eucalyptus urophylla*, with costs provided in the CGEE.[64] We limited the charcoal and firewood production, assuming their current production. In total, wood production accounted for 3.3% as charcoal and 25% as firewood, with the remainder comprising lumber, wood, and other secondary products.[65] With trees spaced 3 × 3 m, the total potential per area is 358.81 GWh/km^2.

To model e-methanol production, we considered a synthetic fuel pathway based on the catalytic hydrogenation of CO_2 derived from ethanol fermentation. The process requires two primary inputs: green H_2 and biogenic CO_2. We assumed the production of e-methanol follows a stoichiometric ratio in which 1 ton of methanol requires 187.5 kg of hydrogen and 1,375 kg of CO_2.[66] Methanol is expressed in liters, with a conversion factor of 0.7918 kg/L. The biogenic CO_2 is assumed to originate from sugarcane-based ethanol production, primarily used to supply light-duty vehicle demand. During fermentation, each ton of ethanol generates approximately 950 kg of CO_2.[67]

In the power and hydrogen sector, we assumed costs given by the EPE[18] for conventional and mature technologies, such

as hydropower plants, combined cycle gas turbine (CCGT), and nuclear. For onshore wind and solar farms, rooftop PV, and batteries, we considered costs for 2050 reported by the NREL.[20] For offshore wind farms, we estimated the costs based on equations compiled by Tavares et al.[68] and considered a reduction of 50% by 2050.[69] Reservoirs, batteries, and hydrogen technologies were considered storage systems in our model, providing alternatives to fossil-fuel-based backup solutions and minimizing curtailments or instability issues (Table S13).

For existing solar technologies, we considered a single variable in our model called *pv_existing*. To find out the current installed capacity of rooftop PV by zone, we aggregated the PV's capacity for every city[70] by zone. For this case, we assumed only the future costs of operation. Then we calculated the average opex of *pv_existing* by considering that the current configuration of utility-scale PV equals 36.7% and 63.3% for rooftop PV.

In our model, the time series of variable resources includes turbine or panel efficiency. Data for technology life-cycle emissions of CO_{2equiv} are based on the IPCC Fifth Assessment Report.[71] This work compares life-cycle emissions from natural gas and offshore wind farms. While hydropower plants can also exhibit substantial life-cycle emissions, it was assumed that no change to the hydropower fleet was made, and total energy sector emissions were not accounted for; thus, these emissions could be excluded from the analysis.

Time series of renewable energy and maximal capacity

RE resources are highly variable over a year and between years. To analyze the weather variability, we considered two decades of data for the baseline and net-zero scenarios. For the hydropower potential, we relied on the observed hydro resources from existing hydropower plants, and for wind and solar time series, we used reanalysis data from NASA's MERRA-2.[72]

Hydropower

We used 20 years of affluent natural energy (ANE) data from the National Operator of the Power System (ONS).[73] The ONS determines ANE using two inputs: natural flow (Q_{nat}) given in m^3/s and the average production (ρ) of the turbine-generator ensemble linked to the elevation difference between the water level associated with 65% of the usable water volume in the upstream reservoir and the water level at tailrace, given in $MW/m^3/s$. Here, i is the hydropower plant, n represents the number of hydropower plants in a basin, and t indicates the period:

$$ANE = \sum_{i=1}^{n} Q_{nat}(i,t).\rho(i). \quad \text{(Equation 2)}$$

Hydropower plants are in groups of basins, and we split the hydropower time series into run-of-river and reservoir based on the installed capacity of both technologies.

The raw hydro time series relies on the installed capacity when data are collected, capturing the effects of changes to the hydropower fleet through time. To obtain an estimate of how the current fleet would have performed through these 20 years, the observed data were multiplied by the ratio of current installed capacity to the capacity at each past moment. Data with negative or missing values were corrected by considering the last non-negative number at the nearest date.

In a reservoir, the remaining ANE can be accumulated over a certain period, working as storage. Table S14 shows the security level for reservoirs given by the ONS.[74]

Wind power

We simulated 20 years (2000–2019) of wind power generation through Renewables.Ninja,[75–77] a platform based on reanalysis data from MERRA-2. Bias correction using data assimilation aimed to reduce or remove systematic errors by comparing the data outputs with observed or already corrected data, bringing them closer to the real values. To correct the bias of offshore nodes, we simulated capacity factors of existing onshore wind farms near the sea and compared them to actual capacity factors, as indicated in a previous work.[78] For onshore wind farms, we used data from the Brazilian Wind Atlas[79] to compare with the simulated reanalysis data due to the absence of existing wind farms in some regions of Brazil.

The Brazilian Wind Atlas provides the already corrected parameters k and c of the Weibull distribution for 2013 at an annual resolution. We generated synthetic wind speed and calculated the probability of different wind speed events with these factors. The Weibull density is estimated by Equation 3:[80]

$$f(v) = \frac{k}{c}\left(\frac{v}{c}\right)^{k-1} \exp\left[-\left(\frac{v}{c}\right)^{k}\right], \quad \text{(Equation 3)}$$

where factor k (unidimensional) describes the shape of the Weibull distribution and factor c indicates the scale in m/s. Low values of k suggest a high frequency of low wind speed, while low values of c mean that the distribution is concentrated around a narrower range of wind speeds (see Figure S10). Figures S11 and S12 present the c and k factors, respectively.

The turbine power production (Pt) is represented by Equation 4:[80]

$$Pt = \int P(v)f(v).dv, \quad \text{(Equation 4)}$$

where $P(v)$ is the turbine power curve. While turbine models are typically chosen for specific projects, for our analysis, we chose recent commercial models with available data on Renewables.Ninja. We considered turbines from Vestas V150 4MW and a hub height of 120 m for onshore wind farms and a larger turbine for offshore wind farms, Vestas V164 8MW, and a height of 100 m. We adopted a resolution of 0.5° × 0.625° (latitude × longitude) for the wind simulation, which is the same resolution as MERRA-2 (see Figure S13A).

The maximal installed capacity results from land availability (km^2) multiplied by a capacity density (MW/km^2). We assumed an installed capacity of 3.56 MW/km^2 for onshore wind farms and 5.2 MW/km^2 for offshore wind, calculated based on an average distance between the turbines of 10D and 5D in an x-y axis,[48] in which the D is the rotor diameter.

Solar power

Similar to the wind simulation, we obtained solar data from MERRA-2 and the interface Renewables.Ninja, which provides solar power outputs from interpolated grid cells and estimates irradiance on the plane of the PV. Generally, the largest annual

irradiation levels are obtained when the tilt of PV modules is equal to the site latitude and when the module faces to the north, in the Southern Hemisphere (azimuth = 0°).[81] PV modules have tilts equal to the local latitude for each coordinate point. We corrected the solar reanalysis data using the solar atlas provided by INPE,[82] which covers 16 years (2000–2015) with monthly resolution. We used solar irradiation on every node's inclined plane (same as the latitude). For additional details on the solar bias correction, see Figure S13B.

The capacity factor output from PV panels can be calculated by multiplying the solar radiation incident on the tilted panels by the panel's parameters and dividing it by its rated power, as indicated in Equation 5:

$$CF = \frac{H * A * eff * L}{RP}, \quad \text{(Equation 5)}$$

where CF is the capacity factor, H is the solar radiation on the tilted panel (Wh/m^2), A is the area of the panel (m^2), eff is the panel's efficiency, L is the coefficient for losses, and RP is the panel's rated power (Wp). We considered panels with an area of 1.6 m^2, an efficiency of 16%, a rated power of 260 Wp, and a loss coefficient of 0.9 (i.e., 10% losses in the PV system). For solar utility-scale PV, we applied the capacity area of 79 MWp/km^2,[49] while for rooftop PV, we assumed a density of 162.5 MWp/km^2.

For rooftop PV, we assumed the surface availability in m^2/household given by region of Brazil,[83] which considers a set of adjustment coefficients that account for physical and structural constraints affecting PV deployment. These coefficients include cc (size factor) and co (orientation factor). Additionally, for apartment buildings, we included cs (shading factor), to account for the reduction in usable area due to shading effects from surrounding structures, and cf (rooftop occupation factor), to reflect the space occupied by essential rooftop installations such as water tanks and HVAC systems. These coefficients were applied to estimate the total effective rooftop area, which was then multiplied by the number of households estimated by IBGE[84] (Table S15). For offshore technologies, we considered available area for wind farms and their optimal locations from previous work.[78]

Bioenergy

Feedstocks for bioenergy production are variable resources, since they depend on seasonal harvesting. In our work, sugarcane-based ethanol production results from suitable lands for sugarcane crops combined with sugarcane yield and distillery efficiency. We calculated overall productivity in terms of liters per hectare using historical data from the National Supply Company (Conab).[54] We assumed data from four recent harvests (from 2018 to 2022) to include possible changes in sugarcane productivity due to weather variability, agricultural and technological improvements, and sugar prices.

Our estimation was based on the total recoverable sugar (TRS), a measure of quality and payment for sugarcane, which indicates the potential to produce ethanol or sugar (see Tables S16 and S17 for further details). However, several variables that affect ethanol production (e.g., yield, sugarcane variety, weather, soil, etc.) are available only aggregated and at a state level, making it difficult to access the exact productivity at a farm/distillery level. To avoid having a single theoretical value that can overestimate or underestimate the potential, we assumed that low-suitability lands have a yield equal to the first quartile of the dataset at the state level (4,896.87 L/ha). We assigned the median (6,024.62 L/ha) and third quartile (7,343.25 L/ha) to medium- and high-potential lands, respectively. In our estimated yield, we removed today's level of sugar production to avoid food conflict. We included seasonality by considering the first month of the harvest period of the most common sugarcane variety (Table S18) in each state, given by RIDESA Brasil[85] and Embrapa Variedades.[86]

The potential of sugarcane was determined based on the Agroecological Zoning for Sugarcane crops,[22] and its value was derived from historical data. The production of second-generation ethanol and surplus electricity depends on the type of distillery, which can generate either second-generation ethanol or electricity using the by-products of sugarcane. We assumed an annual efficiency improvement rate of 0.09% by the year 2030. We considered the average prices across all states from January 2019 to January 2022 to estimate the sugarcane model's inputs.

Corn cultivation for energy purposes requires larger areas than sugarcane, which can significantly impact food production if consumption increases at a large scale.[87] To avoid this, we limited corn production for biofuels, considering its current production. Yet, we defined the corn crop for energy purposes to be available in the off-season of other main growing of existing crops, with the harvest period varying by region. The most recent harvest (2022–23) resulted in 126.4 million tonnes of corn, and 4.9% of this production was used to produce 4.5 billion liters of ethanol.[88] Here, we considered April for harvest in the northeastern region and January and February for the southeast and south, respectively.[89] Agricultural productivity was based on a highly technological farm in Campos Novos, Santa Catarina State, with a production of 10.8 tons/hectare.[56] We assumed a conversion productivity of 400 L of ethanol per tonne of corn.

To estimate the charcoal yield, we assumed the parameters of *Eucalyptus urophylla*, which contains an estimated charcoal potential of 42.5 kg per tree.[90] With tree spacing at 3 × 3 m, the total potential per area is 358.81 GWh/km^2. Here, we assumed that charcoal was invariable over the year.

We assumed no temporal variability for soy oil as feedstock, such as biodiesel, HVO, and SAF.

Demand

Energy demand includes five sectors: industry, transport, building, agriculture, and energy services. The baseline's demand (given by the EPE[18]) is in terms of final energy (the energy supplied to the equipment). To estimate the final energy demand in the what-if scenarios of electrification and net-zero transition, we first determined the useful energy (the energy service required after conversion losses). This value was then multiplied by the efficiency of the corresponding new energy carrier, as expressed in Equation 6:

$$UE_{ijk} = FE_{ijk}.e_{ijk}, \quad \text{(Equation 6)}$$

where the indexes i, j, and k are the carrier, the subsector, and the final use (driving force, heating, direct heating, cooling, lighting, and electrochemical), respectively. The e is the fuel efficiency given by the EPE.[91]

Our assumptions in alternative routes apply to useful energy. The share of final demand may vary depending on changes in total energy demand resulting from efficiency improvements. For instance, we assumed that 75% of the useful demand for rail transportation is met by electricity in limited electrification. However, that becomes 60% when the final energy demand is considered (Table S19). The distribution of demand by subsectors is given by Table S20 and illustrated in Figure S14 for industry, Figure S15 for transport, Figure S16 for building, Figure S17 for agriculture, and Figure S18 for energy. The assumptions are explained in Table S21.

The hourly electricity demand is reported according to the four subsystems by the ONS.[92] To compute the demand profile per zone, we applied the consumption proportion given by distribution companies[93] to the demand. If a distribution company operates in multiple zones, we used a proportion based on the population of each zone.

Our model considers seven carriers (electricity, hydrogen, ethanol, biodiesel, HVO, SAF, and charcoal). We focused exclusively on large-scale biofuels to ensure the computational manageability of our model, assuming that smaller carriers—such as biogas, black liquor, and ancillary biomass—play a role in specific niches or at small scale. We left other carriers out of the model, such as fossil fuels that cannot be replaced with other alternatives (i.e., in some industrial subsectors). However, we considered them in the emission balance.

Emissions

We calculated the emissions and removals associated with the energy sector and the land conversion to dedicated sugarcane crops. For other bioenergy crops like soybean, corn, and charcoal, we assumed that their production did not change land use, as we restricted their cultivation to existing crops. Therefore, their impact on emissions from land-use change was negligible. However, we did consider the emissions derived from their combustion, which were accounted for as biogenic emissions.

We estimated emissions and removals due to land-use change using data on carbon stocks in living biomass (above and below ground) and dead organic matter. We used the "stock-difference approach" for land conversion emissions. The total emission is given by Equation 7:

$$\Delta C = \sum_{ijk} \frac{(C_{t2} - C_{t1})}{t_2 - t_1}, \qquad \text{(Equation 7)}$$

where C is the carbon stock in tons, and the indices are the type of climate (i), type of vegetation (j), and management practice (k). t is the period considered. However, we assumed no temporal variation; instead, we considered the carbon stock by 2050. We calculated the current amount of carbon stored and the potential amount that could be stored if sugarcane crops were implemented. By comparing these two values, we could estimate the difference between them. The specific factors used in calculating carbon stock and the additional CO_2 removal or emission are provided by Araujo et al.[94] and SEEG.[95]

To estimate the carbon stock at t_1, we assumed the current land use. We clipped rasters from MapBiomes[23] in the resulting land for sugarcane crops. To convert a quantity of carbon to the equivalent CO_2, we multiplied the carbon by the ratio of the molecular weight of CO_2 to that of carbon (44/12).

iLUC emissions are associated with expanding pasture and agricultural lands replaced by biofuel feedstock. Here, we considered the iLUC factor of 13 g CO_{2equiv}/MJ for sugarcane ethanol.[96] For soybean-based biofuels in Brazil, specific iLUC values are not well established and are subject to significant uncertainty. To reflect a reasonable range of impacts, we adopted two reference values from global models: 56 g CO_{2equiv}/MJ, derived from the IFPRI-MIRAGE model in a study for the European Commission,[97] and 150 g CO_{2equiv}/MJ, based on the GLOBIOM model.[98] To account for the higher energy yield of HVO compared to conventional biodiesel, we applied a 7% reduction to these iLUC factors, following the methodology proposed by Malins.[99]

We also analyzed the potential of carbon removal by restoring 100% of priority lands for conservation that are currently occupied by human activities and are freed up in terms of energy in scenarios with the LC policy. For that, we also used the "stock-difference approach." We excluded the existing forests, cities, and non-vegetated lands from our analysis. To find the area of each land-use type, we analyzed a land-use raster dataset from Souza et al.[23] within priority lands for conservation.

We also considered the native vegetation types in the biomes and regions to calculate the exact carbon storage impact. We extracted this information from a shapefile provided by ANA,[100] which depicts native vegetation types within priority areas. Using these data, we calculated the area covered by each vegetation type. We applied a weighted average approach to estimate the average carbon stock for each biome and region. This involves assigning weights based on the respective areas of different vegetation types, resulting in a more accurate representation of carbon stock variations across biomes and zones. For further details, see Figure S19.

Annual CO_2 removals by reforesting were estimated with the stock-difference method, using the biomass-increment (in tCO_2/ha year^{-1}) data reported to the IPCC in Brazil's Fourth National Communication.[94] The analysis compares the current land use ("before") with the potential areas converted to forest ("after").

We calculated the emissions from fuel combustion of all sectors. The emissions associated with the power sector include both natural gas combustion in CCGT and the life-cycle emissions of renewable technology manufacturing. Emissions from biofuels are reported as biogenic emissions (i.e., reabsorbed by plants).

We considered emission factors of CO_2, CH_4, and N_2O from the Fourth National Communication of Brazil.[94] Then, we converted them in terms of CO_{2equiv}, considering a global warming potential (GWP) of 1 for CO_2, 25 for CH_4, and 298 for N_2O. For specific factors related to aviation, see Table S22.

RESOURCE AVAILABILITY

Lead contact

Requests for further information and materials should be directed to the lead contact, Paula Conde Santos Borba (paula.borba@inpe.br).

Materials availability

All model outputs are openly available at Zenodo: https://doi.org/10.5281/zenodo.10600013. The power system model can be accessed at Zenodo: https://doi.org/10.5281/zenodo.8020907 and the bioenergy model at Zenodo: https://doi.org/10.5281/zenodo.8020971. Installed capacities across multiple scenarios are also available through our interactive web application: https://energy.ita.br.

Data and code availability

The dataset is publicly available at https://doi.org/10.5281/zenodo.10366868.

ACKNOWLEDGMENTS

P.C.S.B. acknowledges support for the research of this work from funder Coordenação de Aperfeiçoamento de Pessoal de Nível Superior – Brasil (CAPES) – Finance Code 001. This study was financed in part by the São Paulo Research Foundation (FAPESP), grant number 2024/02007-7.

AUTHOR CONTRIBUTIONS

P.C.S.B. conceptualized the study, developed the modeling framework, performed the analysis, and wrote the original draft. W.C.S. supervised the research design and contributed to the validation of the modeling approach. S.P. supervised the research design, contributed to the modeling framework, data processing, and visualization. All authors reviewed and edited the paper.

DECLARATION OF INTERESTS

The authors declare no competing interests.

SUPPLEMENTAL INFORMATION

Supplemental information can be found online at https://doi.org/10.1016/j.oneear.2025.101520.

Received: October 29, 2024
Revised: March 15, 2025
Accepted: October 27, 2025
Published: November 10, 2025

REFERENCES

1. Fuso Nerini, F., Tomei, J., To, L.S., Bisaga, I., Parikh, P., Black, M., Borrion, A., Spataru, C., Castán Broto, V., Anandarajah, G., et al. (2017). Mapping synergies and trade-offs between energy and the sustainable development goals. Nat. Energy *3*, 10–15. https://doi.org/10.1038/s41560-017-0036-5.
2. Goldemberg, J., Coelho, S.T., and Guardabassi, P. (2008). The sustainability of ethanol production from sugarcane. Energy Policy *36*, 2086–2097. https://doi.org/10.1016/j.enpol.2008.02.028.
3. Ioannidis, R., and Koutsoyiannis, D. (2020). A review of land use, visibility and public perception of renewable energy in the context of landscape impact. Appl. Energy *276*, 115367. https://doi.org/10.1016/j.apenergy.2020.115367.
4. Turkovska, O., Castro, G., Klingler, M., Nitsch, F., Regner, P., Soterroni, A.C., and Schmidt, J. (2021). Land-use impacts of brazilian wind power expansion. Environ. Res. Lett. *16*, 024010. https://doi.org/10.1088/1748-9326/abd12f.
5. Convention on Biological Diversity (CBD), Brazil – Country Profile. Available at: https://www.cbd.int/countries/profile/?country=br, [Online; accessed 05-March-2023] .
6. Federative Republic of Brazil, Paris Agreement Nationally Determined Contribution (NDC). Available at: https://unfccc.int/sites/default/files/NDC/2022-06/Updated%20-%20First%20NDC%20-%20%20FINAL%20-%20PDF.pdf (Online; accessed: 11 March 2023).
7. Grangeia, C., Santos, L., and Lazaro, L.L.B. (2022). The brazilian biofuel policy (renovabio) and its uncertainties: An assessment of technical, socioeconomic and institutional aspects. Energy Convers. Manag. X *13*, 100156. https://doi.org/10.1016/j.ecmx.2021.100156.
8. Ramirez Camargo, L., Castro, G., Gruber, K., Jewell, J., Klingler, M., Turkovska, O., Wetterlund, E., and Schmidt, J. (2022). Pathway to a land-neutral expansion of brazilian renewable fuel production. Nat. Commun. *13*, 3157. https://doi.org/10.1038/s41467-022-30850-2.
9. Brannstrom, C., Gorayeb, A., de Sousa Mendes, J., Loureiro, C., Meireles, A.J.d.A., Silva, E.V.d., Freitas, A.L.R.d., and Oliveira, R.F.d. (2017). Is brazilian wind power development sustainable? insights from a review of conflicts in ceará state. Renew. Sustain. Energy Rev. *67*, 62–71. https://doi.org/10.1016/j.rser.2016.08.047.
10. Neri, M., Jameli, D., Bernard, E., and Melo, F.P.L. (2019). Green versus green? adverting potential conflicts between wind power generation and biodiversity conservation in brazil. Perspectives in Ecology and Conservation *17*, 131–135. https://doi.org/10.1016/j.pecon.2019.08.004.
11. MMA, Áreas especiais, http://mapas.mma.gov.br/i3geo/datadownload.htm, [Online; accessed 20-March-2021] (2020).
12. Collins, S., Deane, J.P., Poncelet, K., Panos, E., Pietzcker, R.C., Delarue, E., and Ó Gallachóir, B.P. (2017). Integrating short term variations of the power system into integrated energy system models: A methodological review. Renew. Sustain. Energy Rev. *76*, 839–856. https://doi.org/10.1016/j.rser.2017.03.090.
13. Schmidt, J., Cancella, R., and Pereira, A.O. (2016). An optimal mix of solar pv, wind and hydro power for a low-carbon electricity supply in brazil. Renew. Energy *85*, 137–147. https://doi.org/10.1016/j.renene.2015.06.010.
14. Dranka, G.G., and Ferreira, P. (2018). Planning for a renewable future in the brazilian power system. Energy *164*, 496–511. https://doi.org/10.1016/j.energy.2018.08.164.
15. Rochedo, P.R.R., Soares-Filho, B., Schaeffer, R., Viola, E., Szklo, A., Lucena, A.F.P., Köberle, A.C., Davis, J.L., Rajão, R., and Rathmann, R. (2018). The threat of political bargaining to climate mitigation in brazil. Nat. Clim. Change *8*, 695–698. https://doi.org/10.1038/s41558-018-0213-y.
16. Mahlknecht, J., González-Bravo, R., and Loge, F.J. (2020). Water-energy-food security: A nexus perspective of the current situation in latin america and the caribbean. Energy *194*, 116824. https://doi.org/10.1016/j.energy.2019.116824.
17. Kachirayil, F., Weinand, J.M., Scheller, F., and McKenna, R. (2022). Reviewing local and integrated energy system models: insights into flexibility and robustness challenges. Appl. Energy *324*, 119666. https://doi.org/10.1016/j.apenergy.2022.119666.
18. EPE, Plano nacional de energia 2050 (2020). URL https://www.epe.gov.br/sites-pt/publicacoes-dados-abertos/publicacoes/PublicacoesArquivos/publicacao-227/topico-563/Relatorio%20Final%20do%20PNE%202050.pdf.
19. Pickering, B., Lombardi, F., and Pfenninger, S. (2022). Diversity of options to eliminate fossil fuels and reach carbon neutrality across the entire european energy system. Joule *6*, 1253–1276. https://doi.org/10.1016/j.joule.2022.05.009.
20. NREL, 2023 Annual Technology Baseline (ATB) Cost and Performance Data for Electricity Generation Technologies, https://data.openei.org/submissions/4129, [Online; accessed 01-Sep-2023] (2023).
21. CPTEC, Estações., http://clima1.cptec.inpe.br/estacoes/, [Online; accessed 20-May-2021] (2021).
22. Embrapa, Zoneamento Agroecológico da Cana de açúcar., https://www.embrapa.br/busca-de-solucoes-tecnologicas/-/produto-servico/1249/zoneamento-agroecologico-da-cana-de-acucar, [Online; accessed 08-June-2020] (2009).
23. Souza, C., Zanin Shimbo, J., Rosa, M., Parente, L., Alencar, A., Rudorff, B., Hasenack, H., Matsumoto, M., Ferreira, L., Souza-Filho, P., et al. (2020). Reconstructing three decades of land use and land cover

changes in brazilian biomes with landsat archive and earth engine. Remote Sens. *12*, 12172735. https://doi.org/10.3390/rs12172735.

24. Gazzoni, D.L., Cattelan, A.J., and Nogueira, M.A. (2019). Does the Brazilian soybean production increase pose a threat on the Amazon rainforest?, https://www.infoteca.cnptia.embrapa.br/infoteca/handle/doc/1111175, [Online; accessed 12-Apr-2024].

25. Chen, N., Tsendbazar, N.-E., Requena Suarez, D., Silva-Junior, C.H.L., Verbesselt, J., and Herold, M. (2024). Revealing the spatial variation in biomass uptake rates of brazil's secondary forests. ISPRS J. Photogrammetry Remote Sens. *208*, 233–244. https://doi.org/10.1016/j.isprsjprs.2023.12.013.

26. Oliveira, D.M.S., Cherubin, M.R., Franco, A.L.C., Santos, A.S., Gelain, J.G., Dias, N.M., Diniz, T.R., Almeida, A.N., Feigl, B.J., Davies, C.A., et al. (2019). Jaquelini, Is the expansion of sugarcane over pasturelands a sustainable strategy for brazil's bioenergy industry? Renew. Sustain. Energy Rev. *102*, 346–355. https://doi.org/10.1016/j.rser.2018.12.012.

27. Conab, Safra de grãos é estimada em 313 milhões de toneladas impulsionada pela soja., https://www.gov.br/pt-br/noticias/agricultura-e-pecuaria/2022/11/safra-de-graos-e-estimada-em-313-milhoes-de-toneladas-impulsionada-pela-soja::text=No%20geral%2C%20a%20%C3%A1rea%20semeada,Nacional%20de%20Abastecimento%20(Conab)., [Online; accessed 30-Mar-2023] (2023).

28. Fraanje, T., and Garnett, W. (2020). Soy: Food, Feed, and Land Use Change (Food Climate Research Network).

29. Ministério de Minas e Energia (MME), Empresa de Pesquisa Energética (EPE), Plano Decenal de Expansão de Energia 2034 (PDE 2034), https://www.epe.gov.br/pt/publicacoes-dados-abertos/publicacoes/plano-decenal-de-expansao-de-energia-2034, [Online; accessed 10-Mar-2024] (2023).

30. Lombardi, F., Pickering, B., Colombo, E., and Pfenninger, S. (2020). Policy decision support for renewables deployment through spatially explicit practically optimal alternatives. Joule *4*, 2185–2207. https://doi.org/10.1016/j.joule.2020.08.002.

31. Marengo, J.A., Torres, R.R., and Alves, L.M. (2017). Drought in northeast brazil-past, present, and future. Theor. Appl. Climatol. *129*, 1189–1200. https://doi.org/10.1007/s00704-016-1840-8.

32. Marengo, J.A., Galdos, M.V., Challinor, A., Cunha, A.P., Marin, F.R., Alvalá, R., Alvala, R.C.S., Alves, L.M., Moraes, O.L., Bender, F., and Marengo, R e (09 2021). v i e w a r t i c l e drought in northeast brazil: A review of agricultural and policy adaptation options for food security. Clim. Resil. Sustain. *1*, e17. https://doi.org/10.1002/cli2.17.

33. Material Economics, Industrial Transformation 2050 – Pathways to Net-Zero Emissions from EU Heavy Industry, https://materialeconomics.com/node/13, [Online; accessed 21-May-2023] (2019).

34. Machado, P.G., Hawkes, A., and Ribeiro, C.d.O. (2021). What is the future potential of ccs in brazil? an expert elicitation study on the role of ccs in the country. Int. J. Greenh. Gas Control *112*, 103503. https://doi.org/10.1016/j.ijggc.2021.103503.

35. Becken, S., Mackey, B., and Lee, D.S. (2023). Implications of preferential access to land and clean energy for sustainable aviation fuels. Sci. Total Environ. *886*, 163883. https://doi.org/10.1016/j.scitotenv.2023.163883.

36. Klingler, M., Ameli, N., Rickman, J., and Schmidt, J. (2024). Large-scale green grabbing for wind and solar photovoltaic development in brazil. Nat. Sustain. *7*, 747–757. https://doi.org/10.1038/s41893-024-01346-2.

37. Pfenninger, S., and Pickering, B. (2018). Calliope: a multi-scale energy systems modelling framework. J. Open Source Softw. *3*, 825. https://doi.org/10.21105/joss.00825.

38. Gurobi Optimization, LLC, Gurobi Optimizer Reference Manual (2023). URL https://www.gurobi.com.

39. Delft High Performance Computing Centre (DHPC), DelftBlue Supercomputer (Phase 1), https://www.tudelft.nl/dhpc/ark:/44463/DelftBluePhase1 (2022).

40. Agência Nacional de Água (ANA), Massas d'Água, https://metadados.snirh.gov.br/geonetwork/srv/api/records/7d054e5a-8cc9-403c-9f1a-085fd933610c, [Online; accessed 22-March-2021] (2020).

41. Le Tourneau, F.-M. (2015). The sustainability challenges of indigenous territories in brazil's amazonia. Curr. Opin. Environ. Sustain. *14*, 213–220. https://doi.org/10.1016/j.cosust.2015.07.017.

42. Latinopoulos, D., and Kechagia, K. (2015). A gis-based multi-criteria evaluation for wind farm site selection. a regional scale application in greece. Renew. Energy *78*, 550–560. https://doi.org/10.1016/j.renene.2015.01.041.

43. Ministério do Meio Ambiente (MMA), Áreas Prioritárias para a Conservação, Utilização Sustentável e Repartição dos Benefícios da Biodiversidade Brasileira, https://www.gov.br/mma/pt-br/assuntos/ecossistemas-1/conservacao-1/areas-prioritarias, [Online; accessed 25-Oct-2022] (2018).

44. Empresa de Pesquisa Energética (EPE), Investimentos e custos operacionais e de manutenção no setor de biocombustíveis: 2023 - 2032 (2022). URL https://www.epe.gov.br/sites-pt/publicacoes-dados-abertos/publicacoes/PublicacoesArquivos/publicacao-343/topico-655/NT-EPE-DPG-SDB-2022-07_Investimentos_Custos_O_e_M_Bios_2023-2032.pdf.

45. H. Gasparetto, F. de Castilhos, N. Paula Gonçalves Salau, Recent advances in green soybean oil extraction: A review, J. Mol. Liq. 361 (2022) 119684. doi:https://doi.org/10.1016/j.molliq.2022.119684. URL https://www.sciencedirect.com/science/article/pii/S0167732222012223.

46. A. da Silva César, M. A. Conejero, E. C. Barros Ribeiro, M. O. Batalha, Competitiveness analysis of "social soybeans" in biodiesel production in brazil, Renew. Energy 133 (2019) 1147–1157. doi:https://doi.org/10.1016/j.renene.2018.08.108. URL https://www.sciencedirect.com/science/article/pii/S0960148118310589

47. Turkovska, O., Gruber, K., Klingler, M., Klöckl, C., Ramirez Camargo, L., Regner, P., Wehrle, S., and Schmidt, J. (2024). Methodological and reporting inconsistencies in land-use requirements misguide future renewable energy planning. One Earth *7*, 1741–1759. https://doi.org/10.1016/j.oneear.2024.09.010.

48. S. Pookpunt, W. Ongsakul, Design of optimal wind farm configuration using a binary particle swarm optimization at huasai district, southern thailand, Energy Convers. Manag. 108 (2016) 160–180. doi:https://doi.org/10.1016/j.enconman.2015.11.002. URL https://www.sciencedirect.com/science/article/pii/S0196890415010079.

49. IRENA, Session 2a: Solar power spatial planning techniques, https://www.irena.org/-/media/Files/IRENA/Agency/Events/2014/Jul/15/9_Solar_power_spatial_planning_techniques_Arusha_Tanzania.pdf?la=enhash=F98313D5ADB4702FC910B94586C73AD60FA45FDE, [Online; accessed 05-March-2021] (2014).

50. EPE, Webmap epe. (2023). URL https://gisepeprd2.epe.gov.br/WebMapEPE/.

51. Khatiwada, D., Leduc, S., Silveira, S., and McCallum, I. (2016). Optimizing ethanol and bioelectricity production in sugarcane biorefineries in brazil. Renew. Energy *85*, 371–386. https://doi.org/10.1016/j.renene.2015.06.009.

52. S. I. de Gerenciamento de Recursos Hídricos do Estado de São Paulo, Estudo de impacto ambiental – Sistema de Escoamento Dutoviário de Álcool e Derivados - SEDA., [Online; accessed 08-June-2022] (2009). URL https://sigrh.sp.gov.br/public/uploads/documents/7206/cap-ii-caracterizacao-empreendimento_20abrok.pdf.

53. Kohler, M. (2019). Chapter 19 - economic assessment of ethanol production. In Ethanol, A. Basile, A. Iulianelli, F. Dalena, and T.N. Veziro ğlu, eds. (Elsevier), pp. 505–521. https://doi.org/10.1016/B978-0-12-811458-2.00019-5.

54. Conab, Zoneamento Agroecológico da Cana de açúcar., https://www.conab.gov.br/info-agro/safras/cana, [Online; accessed 10-August-2022] (2022).

55. dos Santos, L.V., de Barros Grassi, M.C., Gallardo, J.C.M., Pirolla, R.A.S., Calderón, L.L., de Carvalho-Netto, O.V., Parreiras, L.S.,

Camargo, E.L.O., Drezza, A.L., Missawa, S.K., et al. (2016). Second-generation ethanol: The need is becoming a reality. Ind. Biotechnol. *12*, 40–57. https://doi.org/10.1089/ind.2015.0017.

56. Conab, custos de produção milho., https://www.conab.gov.br/info-agro/custos-de-producao/planilhas-de-custo-de-producao/itemlist/category/821-milho, [Online; accessed 10-August-2022] (2022).
57. CCEE, Leilão dinâmico. (2022). URL https://www.ccee.org.br/pt/web/guest/-/infoleilao-dinamico-057-dez-2022-19.
58. Leal, M.R.L.V., Walter, A.S., and Seabra, J.E.A. (03 2012). Sugarcane as an energy source. Biomass Convers. Biorefin. *3*, 17–26. https://doi.org/10.1007/s13399-012-0055-1.
59. Jonker, J.G.G., van der Hilst, F., Junginger, H.M., Cavalett, O., Chagas, M.F., and Faaij, A.P.C. (2015). Outlook for ethanol production costs in brazil up to 2030, for different biomass crops and industrial technologies. Appl. Energy *147*, 593–610. https://doi.org/10.1016/j.apenergy.2015.01.090.
60. IEA, Advanced Biofuels – Potential for Cost Reduction , https://www.ieabioenergy.com/wp-content/uploads/2020/02/T41_CostReductionBiofuels-11_02_19-final.pdf, [Online; accessed 22-February-2023] (2023).
61. Capaz, R.S., Guida, E., Seabra, J.E.A., Osseweijer, P., and Posada, J.A. (11 2020). Mitigating carbon emissions through sustainable aviation fuels: costs and potential. Biofuel Bioprod. Biorefining *15*, 502–524. https://doi.org/10.1002/bbb.2168.
62. D. E. Agency, Technology Data, https://ens.dk/en/our-services/projections-and-models/technology-data, [Online; accessed 05-May-2023] (2023).
63. Rodrigues, T., and Braghini Junior, A. (2019). Charcoal: A discussion on carbonization kilns. J. Anal. Appl. Pyrolysis *143*, 104670. https://doi.org/10.1016/j.jaap.2019.104670.
64. Centro de Gestão e Estudos Estratégicos (CGEE), Modernização da produção de carvão vegetal no Brasil: Subsídios para revisão do Plano Siderurgia, https://www.cgee.org.br/web/cgee/busca?q=Moderniza%C3%A7%C3%A3o+da+produ%C3%A7%C3%A3o+de+carv%C3%A3o+vegetal+no+Brasil%3A+Subs%C3%ADdios+para+revis%C3%A3o+do+Plano+Siderurgia%2C [Online; accessed 08-Sep-2022] (2015).
65. IBGE, Produção da extração vegetal e silvicultura (2022). URL https://www.ibge.gov.br/estatisticas/economicas/agricultura-e-pecuaria/9105-producao-da-extracao-vegetal-e-da-silvicultura.html?=t=destaques.
66. Hank, C., Gelpke, S., Schnabl, A., White, R.J., Full, J., Wiebe, N., Smolinka, T., Schaadt, A., Henning, H.-M., and Hebling, C. (2018). Economics carbon dioxide avoidance cost of methanol production based on renewable hydrogen and recycled carbon dioxide – power-to-methanol. Sustain. Energy Fuels *2*, 1244–1261. https://doi.org/10.1039/C8SE00032H.
67. Filho, R.B.d.A., Danielski, L., de Carvalho, F.R., and Stragevitch, L. (2013). Recovery of carbon dioxide from sugarcane fermentation broth in the ethanol industry. Food Bioprod. Process. *91*, 287–291. https://doi.org/10.1016/j.fbp.2012.09.009. https://www.sciencedirect.com/science/article/pii/S096030851200096X.
68. de Assis Tavares, L.F., Shadman, M., de Freitas Assad, L.P., Silva, C., Landau, L., and Estefen, S.F. (2020). Assessment of the offshore wind technical potential for the brazilian southeast and south regions. Energy *196*, 117097. https://doi.org/10.1016/j.energy.2020.117097.
69. Wiser, R., Rand, J., Seel, J., Beiter, P., Baker, E., Lantz, E., and Gilman, P. (05 2021). Expert elicitation survey predicts 37 Nature Energy 2021. Nat. Energy *6*, 555–565. https://doi.org/10.1038/s41560-021-00810-z.
70. EPE, Painel de Dados de Micro e Minigeração Distribuída, https://dashboard.epe.gov.br/apps/pdgd/, [Online; accessed 04-September-2023] (2023).
71. IPCC (2015). Technology-specific Cost and Performance Parameters (Cambridge University Press), pp. 1329–1356. https://doi.org/10.1017/CBO9781107415416.025.
72. Gelaro, R., McCarty, W., Suárez, M., Todling, R., Molod, A., Takacs, L., Randles, C., Darmenov, A., Bosilovich, M., Reichle, R., et al. (2017). The modern-era retrospective analysis for research and applications, version 2 (merra-2). J. Clim. *30*. https://doi.org/10.1175/JCLI-D-16-0758.1.
73. ONS, Data: Carga e geração, http://www.ons.org.br/paginas/energia-agora/carga-e-geracao, [Online; accessed 24-Mar-2022] (2019).
74. ONS, Construção da curva referencial de armazenamento- CREF -para o ano de 2021, https://www.gov.br/mme/pt-br/assuntos/conselhos-e-comites/cmse/atas/2021/anexo-4_nt-ons-dpl-0021-2021-metodologia-curva-referencial-2021.pdf, [Online; accessed 24-Mar-2022] (2021).
75. Pfenninger, S., and Staffell, I. (2016). Long-term patterns of european pv output using 30 years of validated hourly reanalysis and satellite data. Energy *114*, 1251–1265. https://doi.org/10.1016/j.energy.2016.08.060.
76. Staffell, I., and Pfenninger, S. (2016). Using bias-corrected reanalysis to simulate current and future wind power output. Energy *114*, 1224–1239. https://doi.org/10.1016/j.energy.2016.08.068.
77. S. L. Pfenninger S, Renewables Ninja, https://www.renewables.ninja/, [Online; accessed 20-August-2020] (2016).
78. Borba, P.C.S., Sousa, W.C., Shadman, M., and Pfenninger, S. (2023). Enhancing drought resilience and energy security through complementing hydro by offshore wind power—the case of brazil. Energy Convers. Manag. *277*, 116616. https://doi.org/10.1016/j.enconman.2022.116616.
79. Centro de Pesquisas de Energia Elétrica (Cepel), Atlas Eólico Brasileiro – Simulações 2013, https://novoatlas.azurewebsites.net/, [Online; accessed 10-Apr-2021] (2013).
80. de Assis Tavares, L.F., Shadman, M., Assad, L.P.d.F., and Estefen, S.F. (2022). Influence of the wrf model and atmospheric reanalysis on the offshore wind resource potential and cost estimation: A case study for rio de janeiro state. Energy *240*, 122767. https://doi.org/10.1016/j.energy.2021.122767.
81. Mehleri, E.D., Zervas, P.L., Sarimveis, H., Palyvos, J.A., and Markatos, N.C. (2010). Determination of the optimal tilt angle and orientation for solar photovoltaic arrays. Renew. Energy *35*, 2468–2475. https://doi.org/10.1016/j.renene.2010.03.006.
82. Pereira, E., Martins, F., Costa, R., Gonçalves, A., Lima, F., Rüther, R., Abreu, S., Tiepolo, G., Pereira, S., and Souza, J. (2017). Atlas Brasileiro de Energia Solar – 2ª Edição, https://doi.org/10.34024/978851700089, [Online; accessed 12-Apr-2021].
83. Miranda, R.F.C., Szklo, A., and Schaeffer, R. (2015). Technical–economic potential of PV systems on Brazilian rooftops. Renewable Energy *75*, 694–713. https://doi.org/10.1016/j.renene.2014.10.037.
84. IBGE, Número de domícilios, https://sidra.ibge.gov.br/tabela/3033, [Online; accessed 20-November-2020] (2010).
85. Ridesa Brasil, Liberação nacional (2015). URL https://www.ridesa.com.br/_files/ugd/097ffc_630ca4e433634264a1315ef02f4fb1d5.pdf.
86. Embrapa, Variedades, https://www.embrapa.br/agencia-de-informacao-tecnologica/cultivos/cana/pre-producao/caracteristicas/variedades, [Online; accessed 10-Mar-2023] (2022).
87. Dantas, G.A., Legey, L.F.L., and Mazzone, A. (2013). Energy from sugarcane bagasse in brazil: An assessment of the productivity and cost of different technological routes. Renew. Sustain. Energy Rev. *21*, 356–364. https://doi.org/10.1016/j.rser.2012.11.080.
88. Nova cana, Etanol: mercado, https://www.novacana.com/noticias/producao-etanol-milho-cresce-800-cinco-anos-atrai-empresas-270123, [Online; accessed 22-Feb-2023] (2023).
89. Pereira Filho, I. A. (Ed., Cultivo do milho, 9. ed., Sete Lagoas: Embrapa Milho e Sorgo (2015), https://www.infoteca.cnptia.embrapa.br/infoteca/handle/doc/486917, [Online; accessed 10-Mar-2023].
90. de Paula Protásio, T., Roque Lima, M.D., Scatolino, M.V., Silva, A.B., Rodrigues de Figueiredo, I.C., Gherardi Hein, P.R., and Trugilho, P.F. (2021). Charcoal productivity and quality parameters for reliable classification of eucalyptus clones from brazilian energy forests. Renew. Energy *164*, 34–45. https://doi.org/10.1016/j.renene.2020.09.057.
91. Empresa de Pesquisa Energética (EPE), Useful Energy Balance, https://www.epe.gov.br/sites-pt/publicacoes-dados-abertos/publicacoes/

Paginas/Balanco-de-Energia-Util-para-segmentos-selecionados-da-Industria.aspx, [Online; accessed 01-Mar-2023] (2023).

92. Operador Nacional do Sistema Elétrico (ONS), Curva de carga horária, http://www.ons.org.br/Paginas/resultados-da-operacao/historico-da-operacao/curva_carga_horaria.aspx, [Online; accessed 08-Jun-2020] (2020).
93. ANEEL, Relatórios de Consumo e Receita de Distribuição, https://www.aneel.gov.br/relatorios-de-consumo-e-receita, [Online; accessed 06-June-2021] (2019).
94. Brasil. Ministério da Ciência, Tecnologia e Inovações. Secretaria de Pesquisa e Formação Científica, Quarta Comunicação Nacional do Brasil à Convenção-Quadro das Nações Unidas sobre Mudança do Clima, Brasília: Ministério da Ciência, Tecnologia e Inovações, 620 p., ISBN 978-65-87432-18-2, https://www.gov.br/mcti/pt-br/acompanhe-o-mcti/sirene/publicacoes/comunicacoes-nacionais-do-brasil-a-unfccc/arquivos/4comunicacao/4_com_nac_brasil_web.pdf, [Online; accessed 10-Mar-2021] (2020).
95. SEEG, Nota Metodológica: Setor Mudança de Uso da Terra e Florestas (SEEG 12), https://seeg.eco.br/wp-content/uploads/2025/04/SEEG12-NM-MUT-BR.pdf, [Online; accessed 10-Dec-2024] (2024).
96. Maia, R.G.T., and Bozelli, H. (2022). The importance of ghg emissions from land use change for biofuels in brazil: An assessment for current and 2030 scenarios. Resour. Conserv. Recycl. *179*, 106131. https://doi.org/10.1016/j.resconrec.2021.106131.
97. Laborde, D. (2011). Assessing the Land Use Change Consequences of European Biofuel Policies, Tech. Rep. (International Food Policy Research Institute (IFPRI)). commissioned by the European Commission http://re.indiaenvironmentportal.org.in/files/file/biofuelsreportec2011.pdf.
98. Valin, H., Peters, D., van den Berg, M., Frank, S., Havlík, P., Forsell, N., and Hamelinck, C.N. (2015). Land-use change impact of biofuels consumed in the EU, Tech. Rep. 261, Ecofys / IIASA / E4tech, https://energy.ec.europa.eu/publications/land-use-change-impact-biofuels-consumed-eu_en, [Online; accessed 10-Mar-2025].
99. Malins, C. (2020). Soy, Land Use Change and Iluc-Risk: A Review, Tech. Rep. (Cerulogy) https://www.transportenvironment.org/uploads/files/2020_11_Study_Cerulogy_soy_and_deforestation.pdf.
100. ANA, Cobertura Vegetal Nativa do Brasil, https://metadados.snirh.gov.br/geonetwork/srv/api/records/d6f207d-4298-4ff2-9c1e-1cb9f343cd9e, [Online; accessed 20-May-2023] (2004).